Exergoeconomic Analysis and Optimization of CO2 based Novel Combined Cooling and Power Cycles for Engine Waste Heat Recovery

Submitted By

Mohammad Adnan Sami Dinar

200011106

Supervised By

Dr. Mohammad Monjurul Ehsan

A Thesis submitted in partial fulfillment of the requirement for the degree of Bachelor of Science in Mechanical Engineering

Department of Mechanical and Production Engineering (MPE)

Islamic University of Technology (IUT)

October, 2025

<u>Candidate's Declaration</u>

This is to certify that the work presented in this thesis, titled, "**Exergoeconomic Analysis and Optimization of CO2 based Novel Combined Cooling and Power Cycles for Engine Waste Heat Recovery**", is the outcome of the investigation and research carried out by me under the supervision of **Dr. Mohammad Monjurul Ehsan**, Professor, Department of Mechanical and Production Engineering, Islamic University of Technology.

It is also declared that neither this thesis nor any part of it has been submitted elsewhere for the award of any degree or diploma.

Mohammad Adnan Sami Dinar

Student No: 200011106

Recommendation of the Thesis Supervisors

The thesis titled "**Exergoeconomic Analysis and Optimization of CO2 based Novel Combined Cooling and Power Cycles for Engine Waste Heat Recovery**" submitted by **Mohammad Adnan Sami Dinar**, Student No: **200011106** has been accepted as satisfactory in partial fulfillment of the requirements for the degree of B Sc. in Mechanical Engineering **on 29th September, 2025.**

1.

------------------------------------- (Supervisor)
Dr. Mohammad Monjurul Ehsan
Professor
MPE Dept., IUT, Board Bazar, Gazipur-1704, Bangladesh.

CO-PO Mapping of ME 4800 -Theis and Project

COs	Course Outcomes (CO) Statement	(PO)	Addressed by	
CO1	Discover and Locate research problems and illustrate them via figures/tables or projections/ideas through field visit and literature review and determine/Setting aim and objectives of the project/work/research in specific, measurable, achievable, realistic and timeframe manner.	**PO2 Problem analysis**	Thesis Book	√
			Performance by research	√
			Presentation and soft skill	√
CO2	Design research solutions of the problems towards achieving the objectives and its application. Design systems, components or processes that meets related needs in the field of mechanical engineering	**PO3 Design/development of solutions**	Thesis Book	√
			Performance by research	√
			Presentation and soft skill	√
CO3	Review, debate, compare and contrast the relevant literature contents. Relevance of this research/study. Methods, tools, and techniques used by past researchers and justification of use of them in this work.	**PO4 Investigation**	Thesis Book	√
			Performance by research	√
			Presentation and soft skill	√
CO4	Analyse data and exhibit results using tables, diagrams, graphs with their interpretation. Investigate the designed solutions to solve the problems through case study/survey study/experimentation/simulation using modern tools and techniques.	**PO5 Modern tool usage**	Thesis Book	√
			Performance by research	√
			Presentation and soft skill	√
CO5	Apply moral values and research/professional ethics throughout the work, and justify genuine referencing on sources, and demonstration of own contribution.	**PO8 Ethics**	Thesis Book	√
			Performance by research	√
			Presentation and soft skill	√
CO6	Perform own self and manage group activities from the beginning to the end of the research/work as a quality work.	**PO9 Individual work and teamwork**	Thesis Book	√
			Performance by research	√
			Presentation and soft skill	√
CO7	Compile and arrange the work outputs, write the report/thesis, a sample journal paper, and present the work to wider audience using modern communication tools and techniques.	**PO10 Communication**	Thesis Book	√
			Performance by research	√
			Presentation and soft skill	√
CO8	Recognize the necessity of life-long learning in career development in dynamic real-world situations from the experience of completing this project.	**PO12 Life-long learning**	Thesis Book	√
			Performance by research	√
			Presentation and soft skill	√

Student Name /ID:

1.Mohammad Adnan Sami Dinar
200011106

Signature of the Supervisor: …………………………

Name of the Supervisor: Dr. Mohammad Monjurul Ehsan

K-P-A Mapping of ME 4800 -Theis and Project

COs	POs	Related Ks								Related Ps							Related As				
		K1	K2	K3	K4	K5	K6	K7	K8	P1	P2	P3	P4	P5	P6	P7	A1	A2	A3	A4	A5
CO1	PO2	√	√	√	√					√											
CO2	PO3					√				√	√	√				√	√	√	√		
CO3	PO4								√	√	√	√					√	√			
CO4	PO5						√			√				√							
CO5	PO8							√													
CO6	PO9																				
CO7	PO10																				
CO8	PO12																				

Student Name /ID:

1.Mohammad Adnan Sami Dinar
200011106

Signature of the Supervisor: …………………………

Name of the Supervisor: Dr. Mohammad Monjurul Ehsan

List of Sustainable Development Goals (SDGs) Addressed in this Project

SDG No.	Goals	Targets	Relevance to the Thesis	Remarks
1	No Poverty	1.1 Eradicate extreme poverty (people living on less than $1.25/day).		
		1.2 Reduce poverty in all its forms by at least half.		
		1.3 Implement nationally appropriate social protection systems.		
		1.4 Ensure equal rights to economic resources, services, property, inheritance, technology, and financial services.		
		1.5 Build resilience of the poor and reduce exposure to climate-related and other shocks.		
		1.a Mobilize resources to end poverty.		
		1.b Create pro-poor policy frameworks.		
2	Zero Hunger	2.1 End hunger and ensure access to safe, nutritious food year-round.		
		2.2 End all forms of malnutrition.		
		2.3 Double agricultural productivity and incomes of small-scale producers.		
		2.4 Ensure sustainable food production systems and resilient agricultural practices.		
		2.5 Maintain genetic diversity of seeds, plants, and animals.		
		2.a Increase investment in rural infrastructure, research, and technology.		
		2.b Correct and prevent trade restrictions/distortions in global food markets.		
		2.c Adopt measures to ensure proper functioning of food commodity markets.		

3	Good Health and Well-Being	3.1 Reduce global maternal mortality ratio.		
		3.2 End preventable deaths of newborns and under-5 children.		
		3.3 End epidemics of AIDS, tuberculosis, malaria, and neglected tropical diseases.		
		3.4 Reduce premature mortality from NCDs and promote mental health.		
		3.5 Strengthen prevention and treatment of substance abuse.		
		3.6 Halve global deaths/injuries from road traffic accidents.		
		3.7 Ensure universal access to sexual and reproductive healthcare.		
		3.8 Achieve universal health coverage.		
		3.9 Reduce deaths from hazardous chemicals, pollution, and contamination.	√	Reduction of exhaust heat
		3.a Strengthen tobacco control (WHO FCTC).		
		3.b Support R&D of vaccines and medicines.		
		3.c Increase health financing and workforce.		
		3.d Strengthen capacity for early warning and risk management.		
4	Quality Education	4.1 Ensure all complete free, equitable, quality primary and secondary education.		
		4.2 Ensure access to quality early childhood development and pre-primary education.		
		4.3 Ensure equal access to affordable technical, vocational, and higher education.		
		4.4 Increase skills for employment and entrepreneurship.		
		4.5 Eliminate gender disparities in education.		
		4.6 Ensure literacy and numeracy for youth and adults.		

		4.7 Ensure learners acquire knowledge/skills for sustainable development.		
		4.a Build and upgrade education facilities that are inclusive and safe.		
		4.b Expand scholarships for developing countries.		
		4.c Increase supply of qualified teachers.		
5	Gender Equality	5.1 End all forms of discrimination against women and girls.		
		5.2 Eliminate violence against women and girls.		
		5.3 Eliminate harmful practices (child, early, forced marriage, FGM).		
		5.4 Recognize and value unpaid care and domestic work.		
		5.5 Ensure women's participation in leadership and decision-making.		
		5.6 Ensure universal access to reproductive health and rights.		
		5.a Undertake reforms to give women equal rights to resources.		
		5.b Enhance use of enabling technology to empower women.		
		5.c Adopt and strengthen policies and laws for gender equality.		
6	Clean Water and Sanitation	6.1 Achieve universal and equitable access to safe drinking water.		
		6.2 Achieve access to adequate sanitation and hygiene.		
		6.3 Improve water quality by reducing pollution.		
		6.4 Increase water-use efficiency and sustainable withdrawals.		
		6.5 Implement integrated water resources management.		

		6.6 Protect and restore water-related ecosystems.		
		6.a Expand international cooperation in water and sanitation.		
		6.b Support participation of local communities.		
7	Affordable and Clean Energy	7.1 Ensure universal access to affordable, reliable, modern energy services.	√	Low-Cost Energy
		7.2 Increase substantially the share of renewable energy.	√	Recovery of waste heat
		7.3 Double global rate of improvement in energy efficiency.	√	Optimized for Efficiency
		7.a Enhance international cooperation on clean energy research/technology.	√	Recovery of diesel engine waste
		7.b Expand infrastructure and upgrade technology for sustainable energy.	√	Compact and enhanced power cycle
8	Decent Work and Economic Growth	8.1 Sustain per capita economic growth.	√	Lower energy cost
		8.2 Achieve higher levels of productivity through diversification, tech, and innovation.	√	Novel cogeneration cycles
		8.3 Promote policies for decent job creation and entrepreneurship.	√	Requires skilled operators
		8.4 Improve resource efficiency in production and consumption.	√	Optimized efficiency and utilization factor
		8.5 Achieve full and productive employment for all.		

		8.6 Substantially reduce youth not in employment/education/training.		
		8.7 Eradicate forced labour, modern slavery, and child labour.		
		8.8 Protect labour rights and safe working environments.		
		8.9 Promote sustainable tourism.		
		8.a Increase aid for trade support.		
		8.b Develop a global youth employment strategy.		
9	Industry, Innovation, and Infrastructure	9.1 Develop quality, reliable, sustainable infrastructure.	√	Systems for waste heat recovery
		9.2 Promote inclusive and sustainable industrialization.		
		9.3 Increase access of SMEs to financial services and integration into value chains.		
		9.4 Upgrade infrastructure for sustainability and resource efficiency.	√	Compact system for cogeneration
		9.5 Enhance scientific research and technology development.	√	Novel systems
		9.a Facilitate sustainable infrastructure in developing countries.		
		9.b Support domestic tech development and value addition.		
		9.c Increase access to ICT and internet.		
10	Reduced Inequalities	10.1 Achieve income growth of bottom 40%.		
		10.2 Empower and promote inclusion regardless of status.		
		10.3 Ensure equal opportunity and reduce inequalities of outcome.		
		10.4 Adopt policies for fiscal, wage, and social protection equality.		

		10.5 Improve regulation of global financial markets.		
		10.6 Ensure enhanced representation in global institutions.		
		10.7 Facilitate safe, regular, and responsible migration.		
		10.a Implement special treatment for developing countries.		
		10.b Encourage development assistance and investment in least developed areas.		
		10.c Reduce remittance costs.		
11	Sustainable Cities and Communities	11.1 Ensure access to adequate, safe, and affordable housing.		
		11.2 Provide sustainable transport systems.		
		11.3 Enhance inclusive urbanization and capacity for planning.		
		11.4 Protect cultural and natural heritage.		
		11.5 Reduce disaster impact and losses.		
		11.6 Reduce environmental impact of cities (air quality, waste).		
		11.7 Provide access to safe, inclusive green/public spaces.		
		11.a Support positive links between urban, peri-urban, rural.		
		11.b Increase disaster risk reduction strategies.		
		11.c Support least developed countries in sustainable building.		
12	Responsible Consumption and Production	12.1 Implement 10-Year Framework on sustainable consumption/production.		
		12.2 Achieve sustainable management and use of resources.		
		12.3 Halve per capita global food waste.		
		12.4 Manage chemicals and waste sustainably.		

		12.5 Substantially reduce waste generation.	√	Reduction in engine waste
		12.6 Encourage companies to adopt sustainable practices.		
		12.7 Promote sustainable public procurement.		
		12.8 Ensure people have relevant information for sustainable development.		
		12.a Support developing countries' scientific and technological capacity.		
		12.b Develop tools to monitor sustainable tourism impacts.		
		12.c Rationalize inefficient fossil-fuel subsidies.	√	Ensure efficient use of diesel fuel
13	Climate Action	13.1 Strengthen resilience and adaptive capacity to climate-related hazards.		
		13.2 Integrate climate measures into national policies.		
		13.3 Improve education and awareness on climate change.		
		13.a Implement UNFCCC commitments (mobilize $100 billion annually).		
		13.b Promote mechanisms for capacity-building in least developed countries.		
14	Life Below Water	14.1 Reduce marine pollution.		
		14.2 Sustainably manage and protect marine ecosystems.		
		14.3 Minimize and address ocean acidification.		
		14.4 Regulate harvesting and end overfishing.		
		14.5 Conserve at least 10% of coastal and marine areas.		
		14.6 Prohibit harmful fisheries subsidies.		

		14.7 Increase economic benefits from sustainable marine resources.		
		14.a Increase scientific knowledge and marine technology transfer.		
		14.b Provide access for small-scale artisanal fishers.		
		14.c Implement international law for oceans.		
15	Life on Land	15.1 Conserve terrestrial and freshwater ecosystems.		
		15.2 Promote sustainable management of forests.		
		15.3 Combat desertification and restore degraded land.		
		15.4 Ensure conservation of mountain ecosystems.		
		15.5 Take urgent action to reduce biodiversity loss.		
		15.6 Promote fair benefit-sharing from genetic resources.		
		15.7 End poaching and trafficking of protected species.		
		15.8 Prevent introduction of invasive alien species.		
		15.9 Integrate ecosystem values into policies/planning.		
		15.a Mobilize resources for biodiversity.		
		15.b Finance sustainable forest management.		
		15.c Support local communities for forest and wildlife.		
16	Peace, Justice and Strong Institutions	16.1 Reduce violence and related death rates.		
		16.2 End abuse, trafficking, and violence against children.		
		16.3 Promote rules of law and equal access to justice.		

		16.4 Reduce illicit financial/arms flows, organized crime.		
		16.5 Reduce corruption and bribery.		
		16.6 Develop effective, accountable institutions.		
		16.7 Ensure inclusive, participatory decision-making.		
		16.8 Broaden participation of developing countries in global governance.		
		16.9 Provide legal identity for all (including birth registration).		
		16.10 Ensure access to information and protect freedoms.		
		16.a Strengthen national institutions for prevention of violence.		
		16.b Promote/enforce non-discriminatory laws and policies.		
17	Partnerships for the Goals	17.1 Strengthen domestic resource mobilization.		
		17.2 Developed countries to implement ODA commitments.		
		17.3 Mobilize additional financial resources.		
		17.4 Assist developing countries with debt sustainability.		
		17.5 Invest in least developed countries.		
		17.6 Enhance access to science, technology, innovation.		
		17.7 Promote environmentally sound technologies.	√	System to recover waste heat
		17.8 Fully operationalize technology bank for LDCs.		
		17.9 Enhance international support for capacity-building.		

		17.10 Promote a universal, rules-based trading system (WTO).		
		17.11 Increase exports of developing countries.		
		17.12 Timely implementation of duty-free, quota-free market access.		
		17.13 Enhance global macroeconomic stability.		
		17.14 Enhance policy coherence for sustainable development.		
		17.15 Respect national policy space.		
		17.16 Enhance global partnerships.		
		17.17 Encourage multi-stakeholder partnerships.		
		17.18 Enhance data capacity of developing countries.		
		17.19 Support capacity-building for sustainable development indicators.		

Acknowledgment

Bismillah Ir-Rahamn n-Ir Raheem

Firstly, we are grateful to ALLAH (SWT), the most merciful and compassionate, for granting us the power and capability to compose this dissertation.

We express our sincere gratitude towards our project supervisor, **Dr. Mohammad Monjurul Ehsan**, Professor, IUT for his diligent and dedicated guidance throughout the unexpected challenges of the project, and for his invaluable advice whenever difficulties arose. His benevolence, compassion, and effective insight at work alleviated our stress in facing unforeseen challenges and enhanced our productivity in personal endeavors.

We would also like to express our deepest gratitude and acknowledgement to **Yasin Khan**, Lecturer, IUT for his unwavering support, invaluable guidance, and encouragement throughout the project.

We extend our gratitude to our family and friends for their unwavering support and encouragement. To our parents, for their unwavering love, faith in us, and steadfast support for our academic pursuits, and to our friends, for their patience and understanding during this arduous path.

Summary

Traditional energy systems that try to generate both power and cooling from engine waste heat often struggle to cool the exhaust gases enough to make full use of the available energy. To solve this, our study develops four new combined power-and-cooling systems that use an improved version of the carbon dioxide (CO_2) power cycle, called the supercritical–transcritical (sCO_2–tCO_2) cycle. This system is especially good at recovering leftover heat from engines.

Each of the four new systems—named STC-VCRS, STC-FT, STC-EE, and STC-EI—uses a different cooling method, including vapor compression, flash tank, and ejector-based refrigeration techniques. We compared these new designs with an advanced reference system that already performs better than most traditional setups for using engine exhaust heat.

We tested how changes in pressure, temperature, and cooling rates affect performance, and also analyzed how much each system costs to operate. Using optimization techniques inspired by natural selection, we found that the STC-EE system gives the best overall performance, while the STC-EI system offers the lowest energy cost. Further optimization showed that all four new systems can achieve lower costs than the reference design.

In particular, the STC-EE system can produce about 16% more useful energy, and the STC-FT system can lower energy costs by about 4% compared to the baseline. The STC-EI system stands out for balancing both power and cooling efficiency—it achieves nearly 15% higher performance, lower costs, a high cooling efficiency, and strong energy recovery.

Overall, our results show that these new CO_2-based cogeneration systems, especially those using ejector technology, can deliver more energy at a lower cost. This makes them a promising and economical option for recovering waste heat from internal combustion engines.

TABLE OF CONTENTS

List of Figures

List of Tables

Abstract

Cogeneration systems built with conventional supercritical CO_2 topping power cycles fail to cool engine exhausts to sufficiently low temperatures. Therefore, in the present study, four novel cogeneration systems are developed using regenerative Supercritical-Transcritical (sCO_2 – tCO_2) as the toping power cycle which has excellent heat recovery characteristics. These supercritical transcritical cogeneration (STC) cycles use Vapor Compression (STC-VCRS), flash tank (STC-FT), ejector enhanced (STC-EE) and ejector injection (STC-EI) refrigeration system for cooling. The STCs are compared against regenerative sCO_2 – tCO_2 cycle (RSTC) which outperforms recompression sCO_2 cycle in internal combustion engine (ICE) exhaust waste heat recovery (WHR) for reference. Parametric analysis is performed to evaluate the impact of pressure ratios, turbine inlet temperatures, evaporator inlet temperature and evaporator mass flow rate on cycle performance. Exergoeconomic performance of the STCs for a particular operational condition is also assessed. Single objective optimization using genetic algorithm (GA) disclosed STC-EE has the highest utilization factor (UF) of 34.91% followed closely by STC-EI. STC-EI also incurs the lowest unit cost, 7.41 \$/GJ. Multi-objective optimization is performed using Non-Dominated Sorting Algorithm (NSGA-II) to find tradeoff between maximum UF and minimum unit cost. A lower minimum cost is found in all four of the STCs than the reference RSTC. STC-EE has 16.22% higher UF and STC-FT has 4.13% lower cost, 7.128 \$/GJ than the reference system at their optimum. STC-EI provides 15.49% improved UF at 2.3% reduced unit cost, 7.264 \$/GJ, a high COP of 4.013 and 62.9% exergy. These findings reveal ejector vapor injection despite its complexity can provide greater output at lower cost in integrated systems. The study also proves STCs can be the economical choice for IC engine WHR.

Keywords: Supercritical CO_2; Transcritical CO_2; Cogeneration; Ejector; Vapor injection; Waste heat recovery; Exergoeconomic; Multi-objective optimization.

Highlights:

- Sustainable design and parametric evaluation of $sCO_2 – tCO_2$ cogeneration cycles
- The cogeneration cycles incorporate ejector and vapor Injection based cooling
- Performed detailed energy, exergy, and exergo-economic analysis of system
- Multi-objective optimization of operational parameters using genetic algorithm
- STC-EI achieves 62.9% exergy efficiency at 7.264 \$/GJ and 4.013 COP

Nomenclatures and Symbol

A	Total surface area (m^2)
c	Cost per unit exergy, (\$/GJ)
c_{total}	Total product unit cost, (\$/GJ)
$\dot{C}$	Exergetic cost rate, (\$/hr)
$\dot{C}_D$	Exergy Destruction cost rate (\$/hr)
$\dot{C}_W$	Exergy cost rate of work input/output (\$/hr)
Ex	Exergy, (kW)
f	Exergoeconomic impact factor, (%)
i_r	Interest rate (%)
n	Number of operation years
P	Pressure, (MPa)
P_0	Ambient Pressure, (MPa)
Q	Rate of heat transfer, (MW)
Q_{evap}	Evaporative cooling load, (MW)

Q_R	Heat input from reactor (MW)
$Q_{Reheater}$	Heat input from reheater (MW)
r	Relative cost difference, (%)
W	Network output, (kW)
Wc	Compressor work input, (kW)
W_{net}	Network output, (kW)
Z	Capital cost, ($)
$\dot{Z}$	Capital cost rate, ($/hr)
ΔP	Pressure drop
ΔT	Temperature difference

Greek symbols

ε	Effectiveness of heat exchanger, (%)
η	Isentropic Efficiency, (%)
γ	Operation and Maintenance factor
τ	Operational hour
Δ	Difference

Subscripts

c	Compressor
ch	Chemical
ph	Physical
p	Primary Nozzle of Ejector
s	Secondary Nozzle of Ejector
n	Nozzle of Ejector
m	Mixing Chamber of Ejector
d	Diffuser of Ejector
ev	Evaporator
ex	Exergy

th	thermal
is	isentropic
out	Outlet
in	Inlet
ref	Refrigeration
0	Ambient state
1,2,3,4…….	State points
Abbreviations	**Meaning**
C1	Compressor 1
C2	Compressor 2
C3	Compressor 3
CEPCI	Chemical Engineering Plant Cost Index
CIOM	Capital Investment, Operational and Maintenance cost
CRF	Capital Recovery Factor
CSP	Concentrated Solar Power
DEARC	Double Effect Absorption Refrigeration Cycle
ERC	Ejector Refrigeration Cycle
EV	Expansion valve
GA	Genetic Algorithm
GWP	Global Warming Potential
HTPC	High Temperature Power Cycle
HTR	High temperature Recuperator
ICE	Internal Combustion Engine
IHX	Intermediate Heat Exchanger
LTPC	Low Temperature Power Cycle
LTR	Low temperature Recuperator
NSGA	Non-Dominated Sorting Algorithm

ODP	Ozone Depleting Potential
RSTC	Regenerative sCO_2 – tCO_2 Cycle
sCO_2	Supercritical CO_2
SLHX	Suction Line Heat Exchanger
SPECO	Specific Exergy Costing Method
STC	Supercritical Transcritical Cogeneration
STC- EI	Supercritical Transcritical Cogeneration- Ejector Injection
STC-EE	Supercritical Transcritical Cogeneration- Ejector Enhanced
STC-FT	Supercritical Transcritical Cogeneration-Flash Tank
T1	Turbine 1
T2	Turbine 2
tCO_2	Transcritical CO_2
UF	Utilization Factor
VCRS	Vapor Compression Refrigeration System
WHE1	Waste Heat Exchanger 1
WHE2	Waste Heat Exchanger 1
WHR	Waste Heat Recovery

1. Introduction

Internal Combustion Engines (ICE) lose greater than half of its combustion heat to jacket water and exhaust gas released at 400°C-700°C [1]. As a method to recover this waste heat, supercritical cycles have earned a lot of attention in literature due to its many advantages over traditional Brayton and Organic Rankine Cycle (ORC). In fluids near critical point the compressor work is low because of high compressibility. The cycle also has a low volume to power ratio. Additionally, regeneration can recover most of the heat from turbine exhaust unlike in a Rankine Cycle [2]. CO_2 is the fluid most commonly used in supercritical cycles found in studies. The critical temperature and pressure of CO_2 are respectively 30.98°C and 7.38MPa [3]. Due to its proximity to ambient temperature supercritical conditions can easily be reached. It is also a non-toxic, non-explosive, non-inflammable fluid with zero Ozone Depleting Potential (ODP) and Global Warming Potential (GWP) of 1. A high density near critical point leads to a space-efficient design of Supercritical CO_2 (sCO_2) and transcritical (tCO_2) systems [4]. The sCO_2 cycles are most applied in nuclear plants, concentrated solar power (CSP) plants and waste heat recovery (WHR).

1.1 Problem Statement and Research Scope

Exhaust gas leaves with much of the energy despite giving some off to the recovery cycle. Dual expansion or dual compression and expansions systems have been built to address these limitations. However, these new systems specialized for WHR ignore the need for cooling in some power plants. Integrated cogeneration systems have been built adequately from recompression and regenerative sCO_2 models in literature. Regenerative sCO_2–tCO_2 cycle using dual expansion and dual compression has been proven superior to conventional systems for engine waste heat recovery. The cycle solves both pinch point problems and turbine inlet temperature mismatch for CO_2 cycle. Increased flow from shared LTR in low pressure stream decreases heat capacity difference. Considering these merits it also has a scope in integrated system where the heat capacity difference can be further minimized by adding refrigerant flow to LTR. Moreover, there has been limited work on sCO_2 cycles integrated to flash tank enhanced VCRS or ejector vapor injection VCRS.

This study addresses these gaps by integrating four different refrigeration system with regenerative sCO_2 - tCO_2 cycle (RSTC) in an attempt to achieve exergy efficient and economical cogeneration. These novel cogeneration models are compared to evaluating which of the refrigeration systems is best suited for the top cycle. Multi objective optimization is performed to determine the individual optimum operating conditions. The results are also used to compare with the reference sCO_2–tCO_2 system to evaluate improvements. Exergy destruction for each component is determined to suggest improvements. The goal of this study is also to determine which of the VCRS cycles performs better in a fully integrated system for engine waste heat recovery as well as to quantify the improvement cogeneration cycle provides over a power cycle.

2. Literature Review

In subcritical and supercritical cycles heat addition takes place respectively at subcritical and supercritical pressures. In case of a transcritical cycle heat rejection pressure is subcritical, but heat addition pressure is supercritical. A vast array of models for sCO_2 cycles are available in literature. Reheating results in higher turbine output and higher heat addition temperature leading to better thermal efficiency. Excluding regeneration leads to waste of enormous heat. So, it is always part of the basic sCO_2 or tCO_2 cycle design. The use of intercooler reduces compressor work and reduces average heat rejection temperature [5],[6],[7]. A large heat capacity difference between high- and low-pressure CO_2 streams often lead to the pinch point problem. Most CO_2 cycle modifications are recommended to resolve this. In recompression cycle, proposed by Freher [2], only a portion of hot side low temperature recuperator (LTR) mass flows into precooler and subsequently to cold side LTR. The flow through main compressor bypasses the LTR hot side. Increased mass flow in high pressure side reduces heat capacity difference [8],[9],[10]. For precompression cycle introduced by Angelino G. [11], pressure is slightly elevated on low pressure side post HTR to reduce heat capacity difference [12]. Split expansion incorporates a turbine before main heat exchanger to split the expansion process and reduce main heat exchanger and reheater load [13],[14]. Partial cooling system [15], a modification of intercooler recompression cycle [16] was also published by Angelino G. [11]. Recompression occurs after first compressor before intercooler in partial cooling system. These modifications can be stacked to improve cycle performance. Wang et al. [14] compared between various combinations of these cycle and obtained best performance from partial cooling cycle for molten salt solar power tower (SPT). Song et al.[17] improved a preheating sCO_2 cycle using regeneration branch to recover waste heat from diesel engine exhaust gas and water-cooling jacket.

Commonly used tCO_2 power cycle configurations are not as complex as sCO_2 cycles. The usual variants use no recuperator, single recuperator and reheater. All of these three variants were compared against ORC and Kalina cycle for low-grade heat source by Meng et al. [18]. Reheated tCO_2 showed the best thermo-economic performance. Low pinch between cooling water and CO_2 often makes tCO_2 cycle impractical. Zeotropic CO_2 mixtures have been studied as transcritical cycle working fluid to solve this by Xia et al. [19]. But such fluids have low thermal stability thus low operating temperature. Pan et al. designed [20] and optimized [21] a novel self-condensing tCO_2 cycle. The cycle increases cooling pinch by increasing the cooler outlet temperature of CO_2 and using a flash-tank for further condensation. The cycle efficiency reached 34.63% with molten salt heat source. The cycle was also proven empirically feasible [22].

2.1 Dual Expansion CO_2 Power Cycles

Three dual expansion systems were developed by Grant Kimzey [23]. The dual expansion and dual flow split cycle could achieved higher net power than steam cycle in comparison by Cho et al. [24] at the cost of increased complexity due to more components. It also exceeded the output of recompression, intercooling and partial heating cycles [24], [25]. Manente et al. [26] found in investigation that dual expansion systems have optimum turbine inlet temperature closer to heat source temperature for 400^o -600^o C operations. As a result, for 1 MW system dual expansion cycle reached 5.8%-9.5% higher heat recovery efficiency than traditional ones.

Researchers have recommended the same for single pressure double and triple expansion tCO_2 cycle. Wu et al. [27] found double expansion and triple expansion tCO_2 cycle more effectively recovers gas turbine waste heat at 250-412^o C and 412-500^o C respectively for corrosive exhaust. Double expansion performs well at above 338° C for both corrosive and non-corrosive exhaust. The net power output increased to 26.3%. In a subsequent study of these tCO_2 systems for 470° C engine waste heart recovery, Wang et al. [28] discovered double stage tCO_2 has 21.51% and 9.21% higher output power than single and triple expansion systems respectively at a lower cost.

Dual expansion cycles are in essence integrations of two sCO_2 or tCO_2 cycles which are limited by having the same pressure ratios. Zang et al.[29] integrated tCO_2 cycle with dual regenerative sCO_2 and tCO_2 cycle in two different layouts (cycle 3 and 4). It was also integrated with a recompression cycle (cycle 2) in another layout and tested against a simple recompression cycle (cycle 1) for IC engine WHR. The pair of cycles in these layouts were allowed different pressure ratios and designed for parallel heat recovery. This ensured better utilization of the two recuperators and waste heat recovery up to the acid dew point of exhaust gas. Regenerative sCO_2–tCO_2 system performed best among the four on optimization.

2.2 Cascaded Technology in sCO_2 Power Cycles

The sCO_2 or tCO_2 cycle can be combined with other cycles in parallel or series/cascade. Cascade combinations are more common in literature. Battista et al.[30] cascaded an ORC cycle with simple sCO_2 cycle and analyzed for 13 different working points under off design conditions. The configuration managed to recover 9% of the mechanical power of an IC engine. Dual compression–dual expansion sCO_2 cycle was combined with a partial heating tCO_2 cycle through both a cascaded precooler and triple-stage parallel heat recovery for gas turbine by Du et al. [31]. The system increased net power by 5.67 MW and thermal efficiency by 12.6%. Turja et al. [32] likewise combined different sCO_2 cycles with tCO_2 and ORC cycle in series. These include: recompression, partial cooling and intercooling recompression cycles. ORC and sCO_2

shares a heat exchanger before intercooler where as tCO_2 and sCO_2 share a heat exchanger before precooler. The combinations have high optimum turbine inlet temperature at 800° C – 850° C. Combined intercooling recompression system outperforms the others by a 2-2.5% increase in efficiency. R245fa was the best fluid for ORC. Turja et al. [33] later combined the same sCO_2 models with two different ORC instead of a tCO_2 and ORC. This time, combined partial cooling system yielded 7994.54 KW power at 53.365% efficiency. The cycle optimum temperature was found to be 600° C – 700° C.

2.3 Advancement in CO_2 Refrigeration Cycles

The properties like high-volumetric heat capacity, non-toxic, non-combustible and negligible GWP that make CO_2 attractive as power cycle fluid makes it appealing in refrigeration cycle as well [34]. It also has high heat of evaporation compared to many synthetic fluids [35]. It was a common refrigerant due to easy availability and management until the advent of freons and R12 in 1930s [36]. It is again being considered as substitute to environmentally harmful CFC and HCFCs. A tCO_2 refrigeration was first developed and laboratory tested for automobile air conditioning by Lorentzen and Pettersen [35] as a benign alternative to CFC. The performance of a Vapor Compression Refrigeration System (VCRS) may be improved by attaching a suction-line heat exchanger (SLHX) to increase cooling capacity [37], [38]. Cooling capacity can also be increased by using flash-tank vapor injection (FTVI) or intermediate heat exchanger (IHX). FT had at least 3.2% higher heat capacity and up to 2.2% higher COP than IHX in a study by Wang et al.[39]. Attaching an intercooler to reduce compressor work is also an option [40]. Replacing expansion valve with an ejector is another way to improve performance of refrigeration. Li and Groll [41] added an ejector enhanced tCO_2 refrigeration system and found 16% improvement in COP over conventional tCO_2 air conditioning system. A dual evaporator dual ejector tCO_2 cycle for supermarket refrigeration was introduced by Liu et al. [42]. The cycle improved COP and exergy efficiency of dual evaporator tCO_2 cycle by at least 15.9% and 15.5% respectively. Vapor injection can further boost the performance of ejector enhanced systems. Bai et al. [43] analyzed an ejector subcooled vapor injection system (ESCVI) and demonstrated 7.7% improvement in COP. An ejector vapor injection tCO_2 refrigeration cycle optimized by Guti´errez et al. [44] had 17.5% improved COP under subcooled operation (-40°C).

2.4 CO_2 based Combined Cooling and Power Cycles

Combined cooling and power systems add a bottoming refrigeration cycle to a top power cycle by either cascading them through a heat exchanger or by completely integrating them. Complete integration involves directing a split sCO_2 flow to the refrigeration cycle and driving the refrigeration cycle using the turbine. This solves the cooling load requirements for the employees and equipment in powerplants and ensured further utilization of recovered waste heat.

In cascade systems heat rejected by cooler in recompression sCO_2 cycle has been used to drive Double Effect Absorption Refrigeration Cycle (DEARC) [45] and Ejector Refrigeration Cycle (ERC) [46] to obtain cooling and power. Bishal et al. [47] develop a multi-generation system cascading three different cycles namely: sCO_2 partial cooling with reheat, multi effect-thermal vapor desalination (ME-TVC) and absorption refrigeration cycle (ARC). The entire system has upto 70% energy efficiency. Bishal et al. [48] also cascaded a recompression sCO_2 cycle with an ARC before precooler, while placing a ORC on parallel for gas turbine waste heat recovery. The resulting system has highest 49.09% EUF and 0.72 COP.

The sCO_2 turbine power has been separately used to drive ejector enhanced VCRS with organic fluid by Pan et al. [49]. Yu et al.[50] integrated a regenerative sCO_2 cycle with simple tCO_2 refrigeration system for shipboard WHR. Energy and exergy efficiencies of respectively 42.42% and 39.05% was obtained at average energy cost of 9.28 $/GJ. However, lowering evaporation temperature also significantly lowered the cooling capacity. Nanzeeba et al. [51] developed a recuperative sCO_2 cycle integrated with a flash tank enhanced VCRS which was also cascaded to a ORC through precooler for shipboard WHR. The resulting system attained 74.95% energy efficiency and 6.89 MW net work. Zhang et al. [52] cascaded a recompression sCO_2 power cycle with a tCO_2 combined power and refrigeration cycle for trigeneration. The obtained exergy efficiency of 62.88% was 12% higher than stand-alone recompression sCO_2 cycle. Power cycles have also been integrated with ejector refrigeration cycle. The proposed system also reduced costs by at least 4.12%. Wang et al. [53] integrated an ORC with ejector refrigeration system and assessed effects of various parameters on the cycle. A trigeneration system integrating ejector enhanced VCRS with sCO_2 power cycle was studied by Wang et al. [54]. Exergy and energy efficiency as high as 32% and 53% respectively were obtained. Optimization and thermos-economic analysis by Li and Wang [55] revealed an ejector enhanced VCRS integrated with sCO_2 recompression cycle had up to 5.87% improvement in exergy for engine waste heat recovery.

3. Description of the System

The cycle proposed by Zhang et al. [29] contains a regenerative sCO_2 - tCO_2 cycle (RSTC) integrated by a shared Low temperature recuperator (LTR) and cooler to ensure optimum engine waste heat extraction. Temperature gradient of sCO_2 ensures efficient heat exchange in waste heat exchanger 1 (WHE1) and waste heat exchanger 2 (WHE2). Moreover, compressing and pumping CO_2 close to its critical state ensures lower power requirement. Increased flow rate at LTR hot side reduces heat capacity difference between cold and hot stream and thus reduces exergy destruction. Schematic diagram for RSTC can be found in **Figure 1(e)**

In this study, four novel supercritical transcritical cogeneration (STC) cycles have been proposed integrating different bottoming refrigeration cycles to the above power cycle through shared LTR, cooler 1 and cooler 2. The bottoming cycles can draw off a portion of the input energy to generate cooling load, increase total output and potentially decrease cost per kilowatt. Schematics for the cycles are shown in **Figure 1.** The high temperature power cycle (HTPC) containing a regenerative sCO_2 cycle shares an LTR and a cooler with the integrated low temperature power cycle (LTPC) which is a tCO_2 cycle to ensure maximum engine waste heat extraction. In HTPC compressed sCO_2 at high pressure and low temperature (2) passes through LTR (3) and high temperature recuperator (HTR) (4) to facilitate more efficient heat exchange. Then it receives a portion of the heat from engine exhaust gas through waste heat exchanger 1 (WHE1). Afterwards the thermal energy of the high temperature and pressure CO_2 (5) is converted to mechanical energy using turbine1 (T1). Low pressure and high temperature CO_2 (6) enters hot side of HTR and mixes with the CO_2 stream at the exit of turbine 2 (T2). In LTPC liquid CO_2 (10a) is pumped to an intermediate pressure (11), receives the remainder of engine exhaust gas heat through waste heat exchanger 2 (WHE2) and converts its thermal energy to mechanical energy passing through turbine 2 (T2) (12-13). The supercritical mixture (8) goes through a common LTR and cooler 1 (9-1). A portion of the supercritical flow enters the compressor (C) (1a). The remaining flow is cooled down to liquid (10) using a cooler (Cooler2) before being passed onto the pump.

3.1 STC-VCRS

Figure 1(a) and **Figure 2(a)** show the schematic and T-s diagram of STC-VCRS. A suction line heat exchanger (SLHX) has been added before cooler2 to ensure heat exchange between sCO_2 and bottoming VCRS. A fraction of sCO_2 flow at the exit of SLHX is throttled to produce low pressure liquid (14). The remaining portion reaches cooler2 to be liquified just like the reference cycle. Low pressure liquid CO_2 is evaporated in an evaporator. This produces a cooling load. Saturated vapor (15) at evaporator exit enters SLHX. There it receives heat from the hot side of SLHX (1b). Superheated low pressure CO_2 (16) is compressed to the turbine exit pressure (17) by compressor2 (C2). Then CO_2 rejoins the power cycles at mixture. SLHX helps reduce some of the cooling load on cooler2 and superheats the saturated vapor. This improves compressor performance and reduces required power.

3.2 STC- FT

The schematic and T-s diagram of STC-FT are displayed **Figure 1(b)** and **Figure 2(b).** Flash Tank VCRS has more cooling load for the same mass flow than normal VCRS which can increase utilization factor (UF). In STC- flash tank (STC-FT) cycle low pressure two-phase CO2 (14) produced after expansion enters FT. The saturated liquid (15) is evaporated to provide cooling. After leaving the evaporator saturated vapor (16) gets compressed by C3 (17) and joins saturated vapor (19) at the exit of FT. The mixture is superheated (21) at SLHX receiving heat from supercritical CO_2. The vapor is then compressed (22) to turbine exit pressure via C2.

3.3 STC- EE

Ejectors can produce the same effect in refrigerant with less equipment than a flash tank cycle. This is evident from T-s diagrams of **Figure 2(c).** In the schematic displayed in **Figure 1(c)** for supercritical transcritical cogeneration - ejector enhanced (STC-EE) liquid CO_2 stream 10 enters primary suction of ejector. It passes through a motive nozzle where it is subjected to a pressure drop. This low pressure draws fluid at primary suction (19). Low pressure CO2 (14) is homogenously mixed with stream 20 in ejector mixing chamber (15). Some of the pressure is recovered when CO_2 passes the diffuser and exits the ejector as liquid-vapor mixture (16). The mixture is separated as saturated liquid (17) and saturated vapor (21) in a flash tank. Saturated liquid loses pressure in expansion valve and turns to two phase CO_2 (18). This passes through the evaporator to provide cooling. Saturated vapor (19) at evaporator exit enters ejector and loses pressure at suction nozzle (20). Saturated vapor at FT exit is compressed (23) to T1 exit pressure at C2 after gaining heat (22) at SLHX.

3.4 STC- EI

Vapor injection between high pressure and low pressure stages improve COP and cooling in both normal VCR and Ejector enhanced VCR. The schematic and T-S diagram of STC with ejector injection (STC-EI) has been provided in **Figure 1(d)** and **Figure 2(d)**. In STC-EI, two phase refrigerant at ejector exit (16) is separated to saturated vapor (21) and liquid (17) like in STC–EE in flash tank 1 (FT1). The liquid is expanded (18) and again separated to saturated vapor (19) and saturated liquid (24) at flash tank 2 (FT2). The vapor from FT2 enters secondary suction nozzle to be depressurized and accelerated. The liquid at FT2 exit is expanded and evaporated (25-26). Saturated vapor at evaporator exit is compressed (27) to ejector exit pressure. Saturate vapor from FT1 is superheated at SLHX (22) and mixed with vapor at C3 exit. This mixture (28) is then pressurized (23) to turbine exit pressure at high pressure C2.

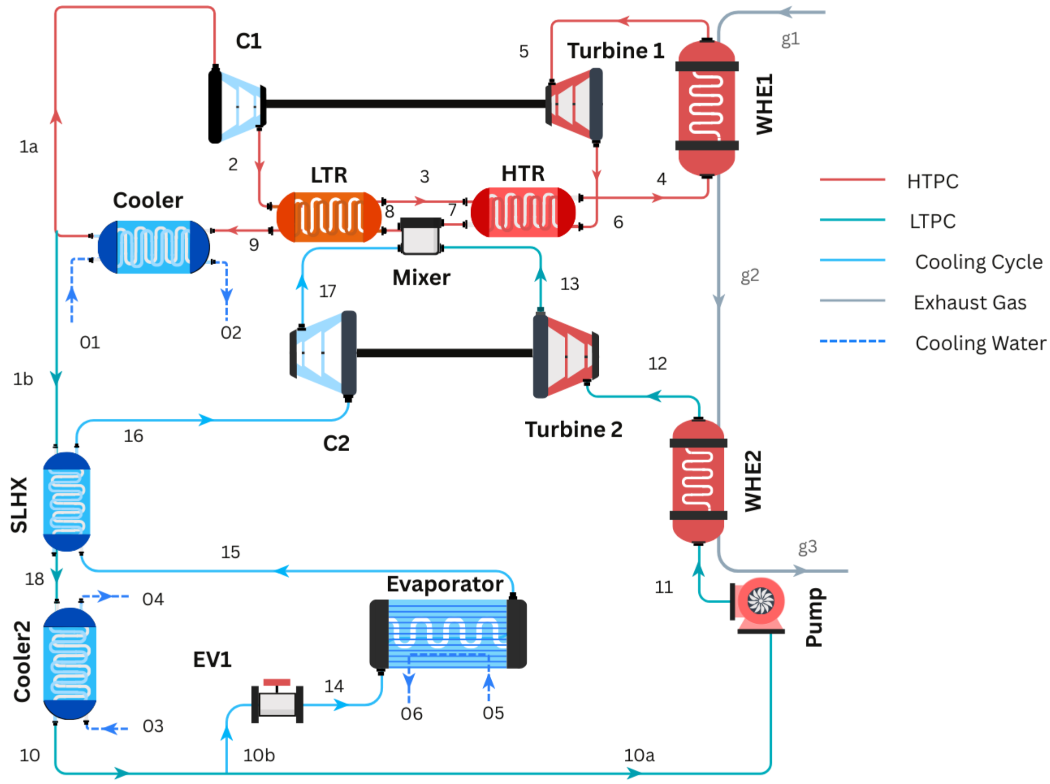
C1
Turbine 1
WHE1
g1
5
1a
2
LTR
3
HTR
4
Cooler
8
7
6
9
Mixer
17
13
01
02
g2
1b
12
16
C2
Turbine 2
WHE2
SLHX
15
g3
18
Evaporator
11
04
Cooler2
Pump
EV1
14
06
05
03
10
10b
10a
HTPC
LTPC
Cooling Cycle
Exhaust Gas
Cooling Water

(a)

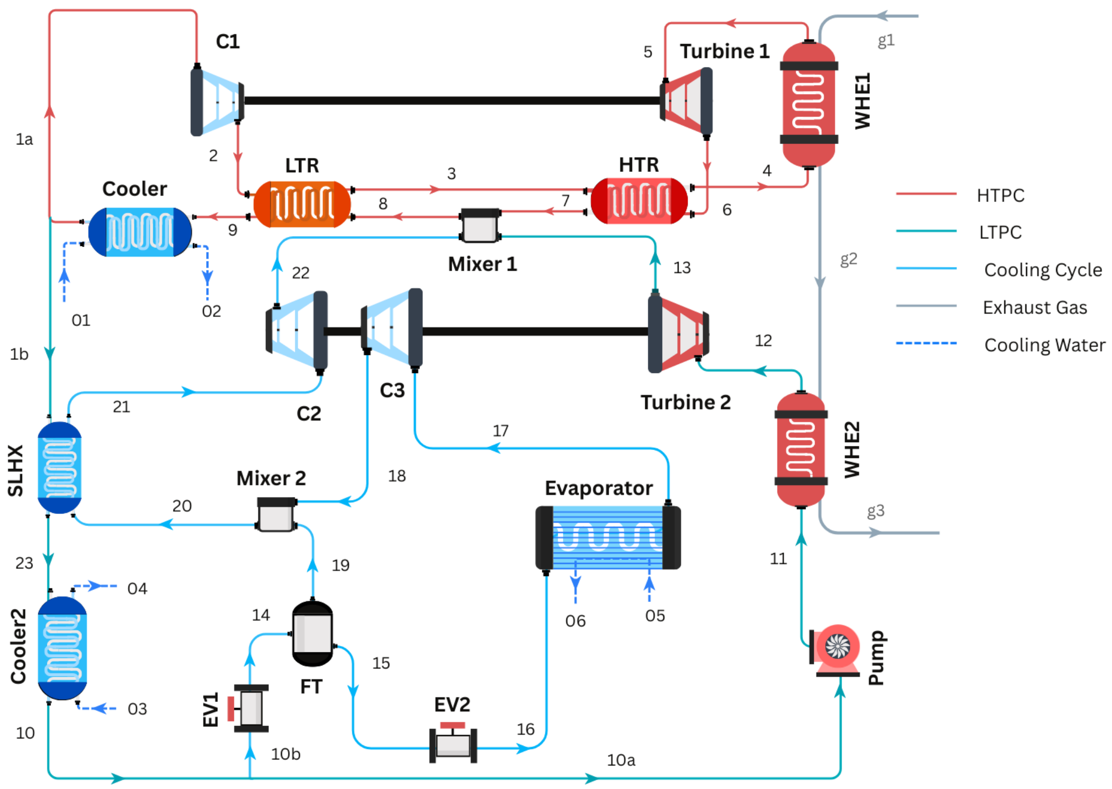
C1
Turbine 1
WHE1
g1
5
1a
2
LTR
3
HTR
4
Cooler
8
7
6
9
Mixer 1
22
13
01
02
g2
12
1b
C3
21
C2
Turbine 2
17
SLHX
Mixer 2
18
Evaporator
WHE2
20
g3
19
11
23
04
14
06
05
15
Cooler2
FT
Pump
EV1
EV2
03
16
10
10b
10a
HTPC
LTPC
Cooling Cycle
Exhaust Gas
Cooling Water

(b)

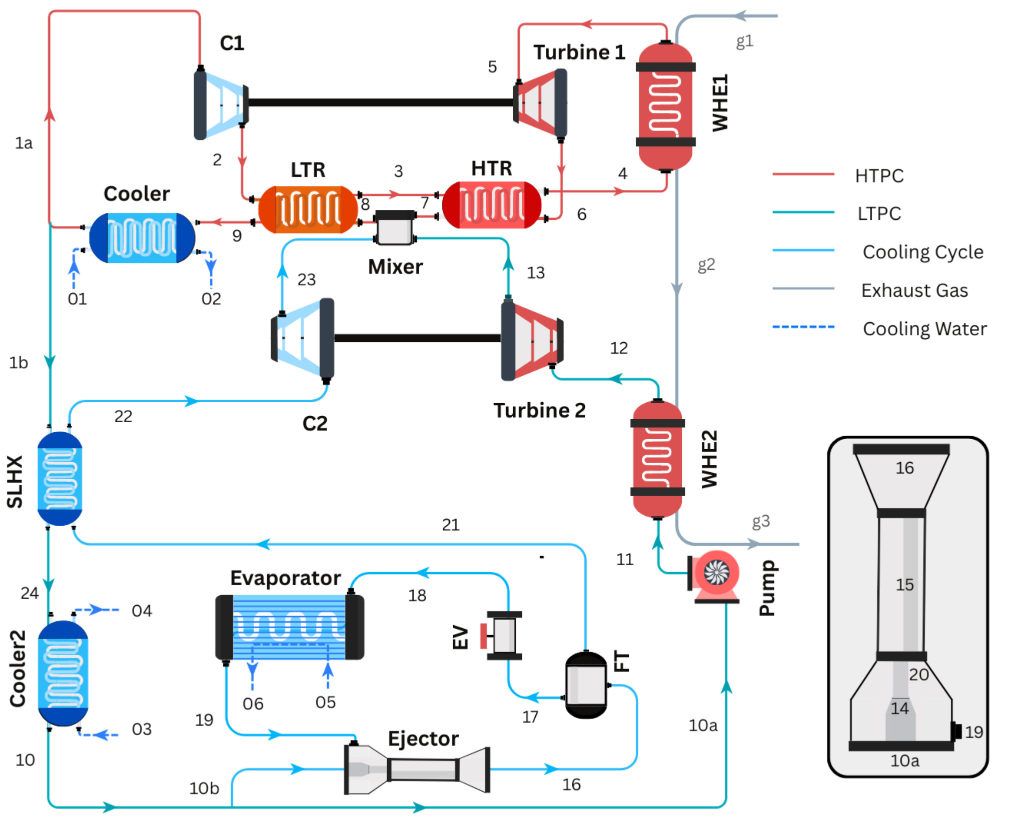
C1
Turbine 1
WHE1
g1
1a
2
3
4
5
6
7
8
9
LTR
HTR
Cooler
Mixer
01
02
23
13
g2
HTPC
LTPC
Cooling Cycle
Exhaust Gas
Cooling Water
12
1b
22
C2
Turbine 2
WHE2
SLHX
21
g3
11
Pump
24
04
Evaporator
18
EV
FT
Cooler2
06
05
17
03
19
10a
Ejector
10
10b
16
15
20
14
19
10a

(c)

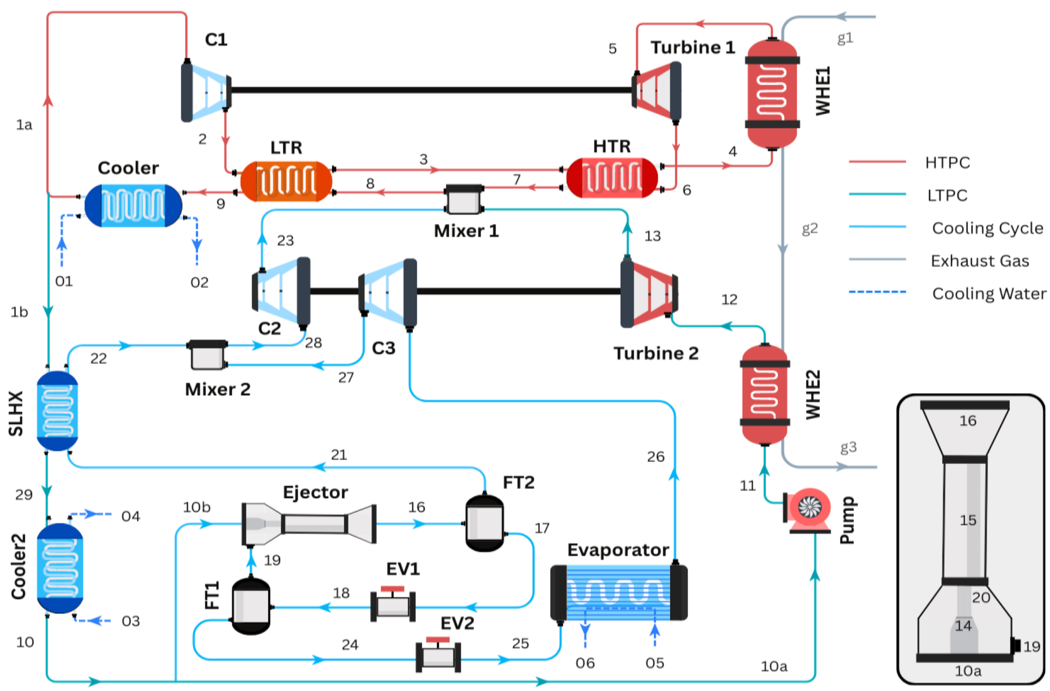
C1
Turbine 1
WHE1
g1
1a
2
5
LTR
HTR
3
4
Cooler
8
7
6
9
Mixer 1
01
02
23
13
g2
HTPC
LTPC
Cooling Cycle
Exhaust Gas
Cooling Water
1b
C2
28
C3
12
22
Mixer 2
27
Turbine 2
WHE2
SLHX
21
26
g3
29
FT2
11
Pump
04
10b
Ejector
16
17
Evaporator
Cooler2
19
EV1
FT1
18
EV2
03
24
25
10
06
05
10a
16
15
20
14
19
10a

(d)

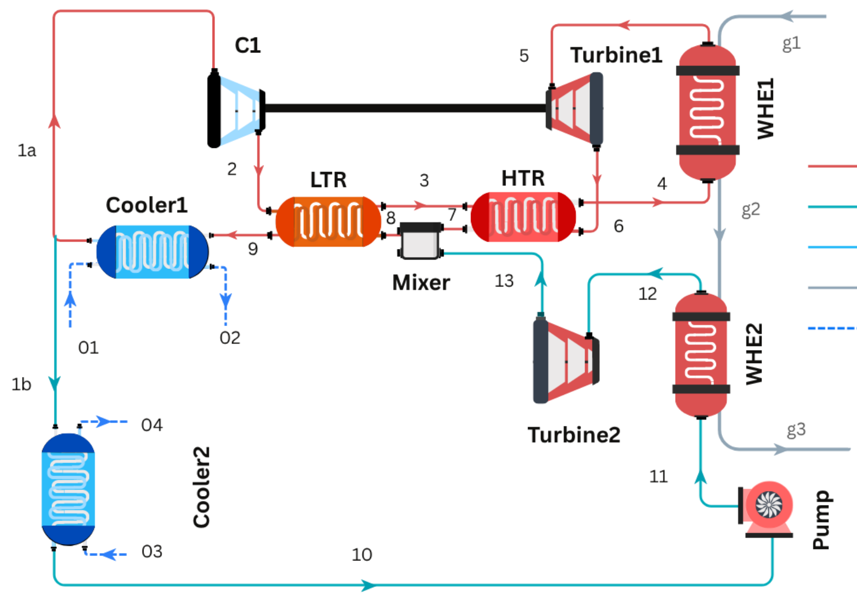

(e)

Figure 1: Schematic diagram of the proposed integrated cycles: (a) STC-VCRS (b) STC-FT (c) STC-EE (d) STC-EI (e) RSTC

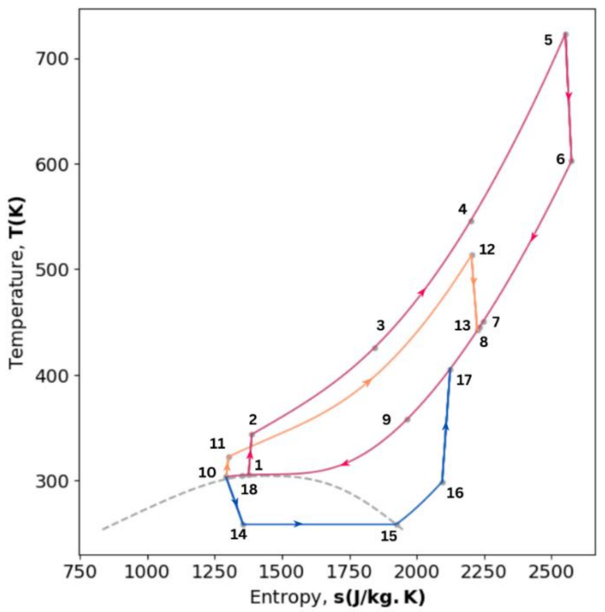

(a)

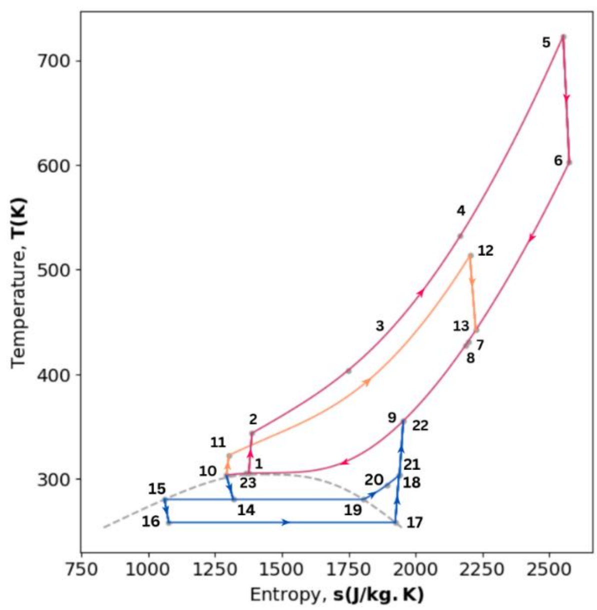

(b)

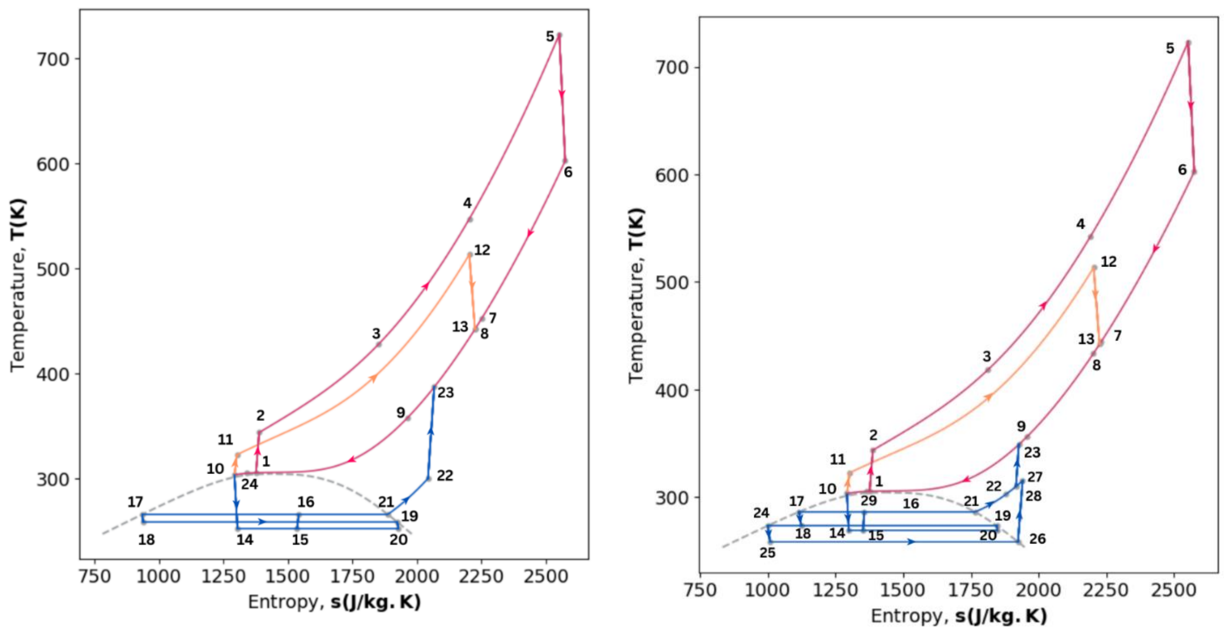

(c) (d)

Figure 2: T-S diagram of the proposed integrated cycles: (a) STC-VCRS (b) STC-FT (c) STC-EE (d) STC-EI.

4. Computational Methodology

In order to evaluate the performance of the proposed system, thermodynamic and economic simulation models are established. To simplify the calculations, the following assumptions are adopted:

- Pressure loss in pipes due to friction is negligible.
- The operating condition of all states of the system is steady.
- The variation in kinetic and potential energy of the working fluid is neglected.
- The working fluid is in a saturated state at evaporator and condenser exits.
- The throttling process in expansion valve is isenthalpic.
- Processes in turbine, pump and compressors are isentropic.
- All heat exchangers are counter-flow types.
- The exhaust temperature must be above 120 °C to avoid acid dew point [29].

4.1 Thermodynamic Model

In Thermodynamic modelling we mainly focus on determining energy and exergy of the system at all states. The mass and energy balance can be defined as [56],

$$\sum \dot{m}_{in} = \sum \dot{m}_{out} \tag{1}$$

$$\sum \dot{Q} - \sum \dot{W} = \sum \dot{m}_{out}\, h_{out} - \sum \dot{m}_{in}\, h_{in} \tag{2}$$

Where, Q and W represent all heat and work interactions in the cogeneration system. Exergy analysis can be defined as the calculation of the irreversibilities and inefficiencies in the system. It characterizes how well the cycle can convert the available incoming thermodynamic power into useful work. The exergy balance equation for all equipment in a steady-state system is given by [57],

$$E_{Q,k} + \sum E_{in,k} = E_{W,k} + \sum E_{out,k} + E_{D,k} \tag{3}$$

The detailed energy and exergy balance equations along with the exergy destruction of STC-EI cycle is listed in **Table 1**.

Net exergy destruction of cogeneration systems can be computed using [58],

$$E_{D,total} = \sum E_{D,k} \tag{4}$$

Further exergy can be quantified into production exergy and fuel exergy. The fuel of a component is defined as all the exergy streams entering it and the product as all the exergy streams removed from it [59]. **Table 3** lists the definitions of the fuel and product of exergy for all components of STC-EI cycle. Alternatively, exergy destruction can be calculated from [60],

$$E_{F,k} = E_{P,k} + E_{D,k} \tag{5}$$

In which $E_{F,k}$ and $E_{P,k}$ are fuel exergy and product exergy, respectively. So, the second law efficiency or exergy efficiency can be expressed by [60],

$$\eta_{Ex,k} = 1 - \frac{E_{D,k}}{E_{F,k}} \tag{6}$$

The total exergy for a stream only incorporates physical and chemical exergies [60], which can be written below:

$$E = E_{ph} + E_{ch} \tag{7}$$

In which E_{ph} and E_{ch} is sited as physical and chemical exergy, respectively. In the present work, concentration of CO2 Is kept constant for the whole process and as a result the chemical exergy does not change from one point to another. Therefore, it has not been taken into consideration.

The physical exergy can be expressed as [61],

$$E_{ph} = \dot{m}[(h - h_0) - T_0(s - s_0)] \tag{8}$$

To find out the area of the heat exchangers, the approximate value of overall heat transfer coefficient is considered [62]. In addition, for the temperature difference of the heat exchangers, logarithmic mean temperature difference is used and can be expressed by [62],

$$\Delta T_{ln} = \frac{(T_{hi}-T_{co})-(T_{ho}-T_{ci})}{\ln[(T_{hi}-T_{co})/(T_{ho}-T_{ci})]} \tag{9}$$

4.2 Ejector Analysis

Constant pressure ejector model outperforms the constant area model as shown in **Figure 3**. So, the model has been chosen for this study. Several assumptions have been made to simulate the ejector. They include:

- Nozzle, diffuser and mixing chamber efficiencies account for the friction loses within the ejector.
- Flow is one – dimensional, homogenous and in equilibrium.
- External heat transfer is negligible.
- Motive and suction fluid reaches same pressure at the exit of the respective nozzle.
- Constant pressure uniform mixing occurs at mixing chamber.

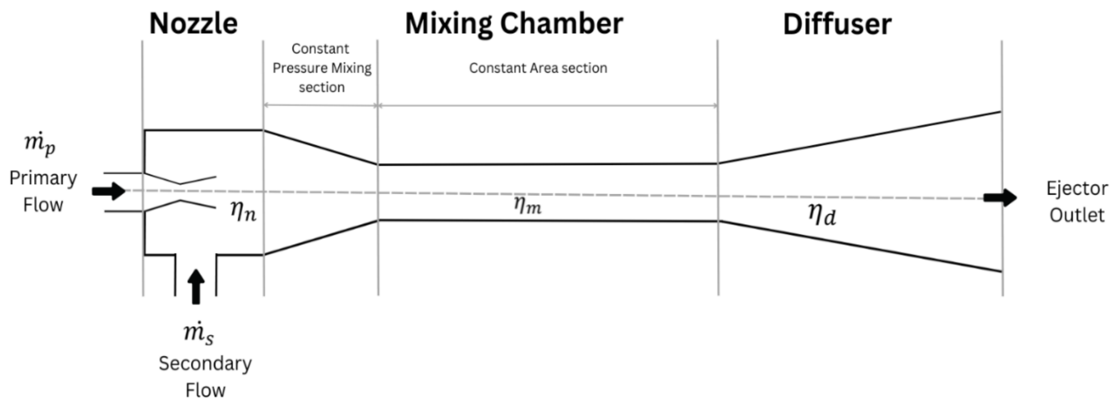

Figure 3: Working process and structure of an ejector.

The most important ejector parameters are secondary nozzle pressure drop and entrainment ratio. For a suction pressure $P_{s,in}$ and exit pressure $P_{s,out}$ pressure drop is,

$$\Delta P = P_{s,in} - P_{s,out} \tag{10}$$

Entrainment ratio is secondary suction and primary motive mass flow ratio:

$$w = \frac{\dot{m}_s}{m_p} \tag{11}$$

Ejector calculations are done in an iterative method initially purposed by Kornhauser [70]. For a given pressure drop ΔP, an initial estimate for entrainment ratio is assumed. This is iteratively updated until there is negligible difference between theoretical and obtained value. Suction and motive fluids are accelerated through separate nozzles, but is designed to achieve equal exit pressure for uniform mixing.

Equations for properties at primary motive nozzle outlet:

Outlet pressure: $$P_{p,out} = P_{p,in} - \Delta P \tag{12}$$

Nozzle efficiency: $$h_n = \frac{h_{p,in} - h_{p,out}}{h_{p,in} - h_{p,out,s}} \tag{13}$$

Outlet velocity:

$$v_{p,out} = \sqrt{2(h_{p\,,in} - h_{p\,,out}\,)} \tag{14}$$

Cross-section Area:

$$A_{p,out} = \frac{1}{(1+w)v_{p,out}\,\rho_{p,out}} \tag{15}$$

Equations for properties at the secondary nozzle outlet:

Outlet pressure:

$$P_{s,out} = P_{s,in} - \,\Delta P \tag{16}$$

Nozzle efficiency:

$$h_n = \frac{h_{s,in} - h_{s,out}}{h_{s,in} - h_{s,out,s}} \tag{17}$$

Outlet velocity:

$$v_{p,out} = \sqrt{2(h_{s\,,in} - h_{s\,,out}\,)} \tag{18}$$

Cross-section Area:

$$A_{s,out} = \frac{1}{(1+w)v_{s,out}\,\rho_{s,out}} \tag{19}$$

Equations for properties at the mixing section outlet:

Outlet Pressure:

$$P_m = P_{p,out} = P_{s,out} \tag{20}$$

Outlet Velocity:

$$v_{m,out} = \frac{\sqrt{\eta_m}}{1+w}\,(\,v_{m,out} + wv_{s,out}) \tag{21}$$

Outlet enthalpy:

$$h_{m,out} = \frac{1}{1+w}\,(h_{p\,,out} + \frac{v_{p,out}^2}{2}) + \frac{w}{1+w}\,(h_{sn\,,out} + \frac{v_{s,out}^2}{2}) - \frac{v_{m,out}^2}{2} \tag{22}$$

Outlet Entropy:

$$s_{m,out} = s(P_m\,, h_{m,out}) \tag{23}$$

Equations for properties at the Diffuser outlet:

Outlet Enthalpy:

$$h_{d,out} = \; h_{m,out} + \frac{v_{m,out}^2}{2} \tag{24}$$

Diffuser efficiency:

$$h_d = \frac{h_{d,out,s} - h_{m,out}}{h_{d,out} - h_{m,out}} \tag{25}$$

Outlet Pressure:

$$P_{d,out} = P(h_{d,out,s}\,, s_{m,out}) \tag{26}$$

4.3 Exergoeconomic Model

Exergoeconomic analysis combines the conventional exergy with thermo-economic performance for each component by relating the purchased equipment cost and thermodynamic efficiency. It is a key factor that provides us with exergetic cost at the level of system components. Among the various exergoeconomic methodologies, in this paper we have used the specific exergy costing method (SPECO) [59]. To conduct this analysis, all energy and exergy streams, as well as the capital investment cost, operational and maintenance cost (CIOM) for all components, were quantified. The cost balance equations based on the exergy flow of the *k*th component can be defined as follows [29]:

$$\sum\dot{C}_{out,k} + \dot{C}_{W,k} = \sum\dot{C}_{in,k} + \dot{C}_{Q,k} + \dot{Z}_k \tag{27}$$

which states that the total cost rate of all exergy outflows ($\sum\dot{C}_{out,k}$) is equal to the sum of the cost rate of all exergy inflows ($\sum\dot{C}_{in,k}$), the capital investment, operating and maintenance costs ($\dot{Z}_k$) [52]. $\dot{C}_{W,k}$ and $\dot{C}_{Q,k}$ are the total cost rate of work output and heat input to the kth component, respectively. The cost rate of the exergy stream can be defined as [60]:

$$\dot{C}_k = c_k\dot{E}_k \tag{28}$$

where c_k is the per unit cost of each exergy flow. The annual levelized CIOM cost rate for the *k*th component can be described as follows [60]:

$$\dot{Z}_k = \dot{Z}_k^{CI} + \dot{Z}_k^{OM} \tag{29}$$

$$\dot{Z}_k^{CI} = Z_k(\mathrm{CRF}/\tau) \tag{30}$$

$$\dot{Z}_k^{OM} = Z_k(\gamma_k/\tau) \tag{31}$$

where τ and γ_k are annual operation hours of 8000 h [29], operation and maintenance coefficient of 0.06 [29], respectively. CRF denotes the capital recovery factor, which can be obtained by:

$$CRF = \frac{i_r(1+i_r)^n}{(1+i_r)^n-1} \tag{32}$$

where n and i_r are 20 years of service time and 12% interest rate [29]. Furthermore, Z_k is defined as the capital cost function for the kth component which is listed in **Table A1**. Besides, the heat from exhaust gases is seen as a free thermal source, so that the levelized exergy cost of the exhaust gas is effectively negligible. The cost rate balance and other auxiliary equations for the STC-EI system components are listed in **Table 2**. The cost balance and auxiliary equations are formed on the basis of Fuel and Product principle of SPECO [59]. The different exergoeconomic behavior was analyzed using several parameters provided in **Table 4**.

The STCs all have a regenerative sCO_2 as the HTPC and a tCO_2 as LTPC. The components in these power cycles are: Turbine 1, WHE1, C1, HTR, LTR, cooler1, cooler2, pump, WHE2, turbine 2 and mixing chamber. Each of these 11 components has been modeled as a control volume to form the energy and exergy balance equations provided in **Table 1**. However, the bottoming refrigeration cycle for the STCs vary. All four systems contain in common at least one: expansion valve, evaporator, a compressor and SLHX. STC-EE contains an ejector and flash tank besides these. STC-FT contains two expansion valves, two FT, two expansion valve, two compressor, one evaporator, SLHX and mixing chamber. In addition to the components in STC-FT, the STC-EI has an ejector. Since STC-EI covers maximum components, energy, exergy, and cost rate balance equations have been provided for this configuration only.

4.4 Performance Evaluation Parameters

Four parameters: Coefficient of Performance (COP), Utilization Factor (UF), Exergy efficiency (η_{Ex}) and product unit cost (c_{total}) are chosen to evaluate the performance of the STCs and compare against RSTC. Performance of the bottoming refrigeration cycle can be quantified through coefficient of power, [52]

$$COP = \frac{\dot{Q}_{ref}}{\dot{W}_c} \tag{33}$$

The total output of the cogeneration system can be evaluated using Utilization Factor [63]

$$UF = \frac{\dot{W}_{net} + \dot{Q}_{ref}}{\dot{Q}_{in}} \tag{34}$$

Here, W_{net} is the net output of the system and Q_{ref} is the net cooling load. $\dot{W}_c$ is the total compressor work done. Refrigeration exergy, total available exergy and Overall system exergy can be defined as [64],

$$\dot{E}_{ref} = \dot{Q}_{ref} \times \left|1 - \frac{T_o}{T_{evp}}\right| \tag{35}$$

$$\dot{E}_{av} = m_g\left(\left(h_{g1} - h_{av}\right) - T_o\left(s_{av} - s_{g1}\right)\right) \tag{36}$$

$$\eta_{Ex} = \frac{\dot{W}_{net} + \dot{E}_{ref}}{\dot{E}_{av}} \tag{37}$$

Here, h_{av} and s_{av} are the enthalpy and entropy of the exhaust gas at the minimum available temperature and T_{evp} is the evaporation temperature. The performance criterion based on the total product unit cost (c_{total}) can be defined as [65]:

$$c_{total} = \sum_{i=1}^{n_k} \frac{\dot{Z}_k}{W_{net} + Q_{ref}} \tag{38}$$

Where n_k is the amount of equipment in each cogeneration cycle.

Table 1: Equations for Energy and Exergy Balance of each component in Ejector Injection [29],[52]

Components	Energy balance	Exergy balance
WHE1	$\dot{Q}_{WHE1} = \dot{m}_4(h_5 - h_4) = \dot{m}_g(h_{g1} - h_{g2})$	$\dot{E}_5 + \dot{E}_{g2} + \dot{E}_{D,WHE1} = \dot{E}_4 + \dot{E}_{g1}$
Turbine1	$\dot{W}_{T1} = \dot{m}_5(h_5 - h_6), h_6 = h_5 - (h_5 - h_{6S})\eta_{T1}$	$\dot{E}_6 + \dot{W}_{T1} + \dot{E}_{D,T1} = \dot{E}_5$
HTR	$\dot{Q}_{HTR} = \dot{m}_3(h_4 - h_3) = \dot{m}_6(h_6 - h_7)$	$\dot{E}_7 + \dot{E}_4 + \dot{E}_{D,HTR} = \dot{E}_6 + \dot{E}_3$
LTR	$\dot{Q}_{LTR} = \dot{m}_2(h_3 - h_2) = \dot{m}_8(h_8 - h_9)$	$\dot{E}_9 + \dot{E}_3 + \dot{E}_{D,LTR} = \dot{E}_8 + \dot{E}_2$
C1	$\dot{W}_C = \dot{m}_2(h_2 - h_1), h_2 = h_1 + (h_{2S} - h_1)/\eta_C$	$\dot{E}_2 + \dot{E}_{D,C1} = \dot{E}_{1a} + \dot{W}_C$
Cooler1	$\dot{Q}_{Cooler1} = \dot{m}_9(h_9 - h_1) = \dot{m}_{01}(h_{02} - h_{01})$	$\dot{E}_1 + \dot{E}_{02} + \dot{E}_{D,Cooler1} = \dot{E}_9 + \dot{E}_{01}$
Cooler2	$\dot{Q}_{Cooler2} = \dot{m}_{10}(h_{29} - h_{10}) = \dot{m}_{03}(h_{04} - h_{03})$	$\dot{E}_{10} + \dot{E}_{04} + \dot{E}_{D,Cooler2} = \dot{E}_{29} + \dot{E}_{03}$
WHE2	$\dot{Q}_{WHE2} = \dot{m}_{11}(h_{12} - h_{11}) = \dot{m}_g(h_{g2} - h_{g3})$	$\dot{E}_{12} + \dot{E}_{g3} + \dot{E}_{D,WHE2} = \dot{E}_{11} + \dot{E}_{g2}$
Turbine2	$\dot{W}_{T2} = \dot{m}_{12}(h_{12} - h_{13}), h_{13} = h_{12} - (h_{12} - h_{13S})\eta_{T2}$	$\dot{E}_{13} + \dot{W}_{T2} + \dot{E}_{D,T2} = \dot{E}_{12}$
Mixer1	$\dot{m}_8 h_8 = \dot{m}_7 h_7 + \dot{m}_{13} h_{13} + \dot{m}_{23} h_{23}$	$\dot{E}_8 + \dot{E}_{D,Mixer1} = \dot{E}_7 + \dot{E}_{13} + \dot{E}_{23}$

SLHX	$\dot{Q}_{SLHX} = \dot{m}_{29}(h_1 - h_{29}) = \dot{m}_{21}(h_{22} - h_{21})$	$\dot{E}_{29} + \dot{E}_{22} + \dot{E}_{D,SLHX} = \dot{E}_{1b} + \dot{E}_{21}$
Pump	$\dot{W}_{Pump} = \dot{m}_{11}(h_{11} - h_{10}), h_{11} = h_{10} + (h_{11S} - h_{10})/\eta_{Pump}$	$\dot{E}_{11} + \dot{E}_{D,Pump} = \dot{E}_{10a} + \dot{W}_{Pump}$
EV1	$h_{17} = h_{18}$	$\dot{E}_{18} + \dot{E}_{D,Exp1} = \dot{E}_{17}$
EV2	$h_{24} = h_{25}$	$\dot{E}_{25} + \dot{E}_{D,Exp2} = \dot{E}_{24}$
Ejector		$\dot{E}_{16} + \dot{E}_{D,Ejector} = \dot{E}_{10b} + \dot{E}_{19}$
Evaporator	$\dot{Q}_{Evap.} = \dot{m}_{25}(h_{26} - h_{25}) = \dot{m}_{05}(h_{05} - h_{06})$	$\dot{E}_{26} + \dot{E}_{06} + \dot{E}_{D,Evap.} = \dot{E}_{25} + \dot{E}_{05}$
C2	$\dot{W}_{C2} = \dot{m}_{26}(h_{27} - h_{26}), h_{26} = h_{26} + (h_{27S} - h_{26})/\eta_{C2}$	$\dot{E}_{27} + \dot{E}_{D,C2} = \dot{E}_{26} + \dot{W}_{C2}$
Mixer2	$\dot{m}_{28}h_{28} = \dot{m}_{27}h_{27} + \dot{m}_{22}h_{22}$	$\dot{E}_{28} + \dot{E}_{D,Mixer2} = \dot{E}_{27} + \dot{E}_{22}$
C3	$\dot{W}_{C3} = \dot{m}_{28}(h_{23} - h_{28}), h_{28} = h_{23} + (h_{28S} - h_{23})/\eta_{C3}$	$\dot{E}_{23} + \dot{E}_{D,C3} = \dot{E}_{28} + \dot{W}_{C3}$

Table 2: Cost rate balance and auxiliary equations for each component of Ejector Injection [29]

Components	**Cost Rate Balance**	**Auxiliary equations**
WHE1	$\dot{C}_5 + \dot{C}_{g2} = \dot{C}_4 + \dot{C}_{g1} + \dot{Z}_{WHE1}$	$\dot{C}_{g2}/\,\dot{E}_{g2} = \dot{C}_{g1}/\dot{E}_{g1}$

Turbine1	$\dot{C}_6 + \dot{C}_{W_{T1}} = \dot{C}_5 + \dot{Z}_{T1}$	$\dot{C}_6/\dot{E}_6 = \dot{C}_5/\dot{E}_5$
HTR	$\dot{C}_7 + \dot{C}_4 = \dot{C}_6 + \dot{C}_3 + \dot{Z}_{HTR}$	$\dot{C}_7/\dot{E}_7 = \dot{C}_6/\dot{E}_6$
LTR	$\dot{C}_9 + \dot{C}_3 = \dot{C}_8 + \dot{C}_2 + \dot{Z}_{LTR}$	$\dot{C}_9/\dot{E}_9 = \dot{C}_8/\dot{E}_8$
C1	$\dot{C}_2 = \dot{C}_{1a} + \dot{C}_{W_C} + \dot{Z}_c$	$\dot{C}_{W_C}/\dot{W}_C = \dot{C}_{W_{T1}}/\dot{W}_{T1}$, $\dot{C}_{1a} = (1 - x_2)\dot{C}_1$
Cooler1	$\dot{C}_1 + \dot{C}_{02} = \dot{C}_9 + \dot{C}_{01} + \dot{Z}_{Cooler1}$	$\dot{C}_{01} = 0$, $\dot{C}_9/\dot{E}_9 = \dot{C}_1/\dot{E}_1$
Cooler2	$\dot{C}_{10} + \dot{C}_{04} = \dot{C}_{29} + \dot{C}_{03} + \dot{Z}_{Cooler2}$	$\dot{C}_{03} = 0$, $\dot{C}_{29}/\dot{E}_{29} = \dot{C}_{10}/\dot{E}_{10}$
WHE2	$\dot{C}_{12} + \dot{C}_{g3} = \dot{C}_{11} + \dot{C}_{g2} + \dot{Z}_{WHE2}$	$\dot{C}_{g3}/\dot{E}_{g3} = \dot{C}_{g2}/\dot{E}_{g2}$
Turbine2	$\dot{C}_{13} + \dot{C}_{W_{T2}} = \dot{C}_{12} + \dot{Z}_{T2}$	$\dot{C}_{13}/\dot{E}_{13} = \dot{C}_{12}/\dot{E}_{12}$, $\dot{C}_{W_{T2}}/\dot{W}_{T2} = \dot{C}_{W_{T1}}/\dot{W}_{T1}$
Mixer1	$\dot{C}_8 = \dot{C}_7 + \dot{C}_{13} + \dot{C}_{23}$	
SLHX	$\dot{C}_{29} + \dot{C}_{22} = \dot{C}_{1b} + \dot{C}_{21} + \dot{Z}_{SLHX}$	$\dot{C}_{29}/\dot{E}_{29} = \dot{C}_{1b}/\dot{E}_{1b}$, $\dot{C}_{1b} = x_2\dot{C}_1$
Pump	$\dot{C}_{11} = \dot{C}_{10a} + \dot{C}_{W_{pump}} + \dot{Z}_{Pump}$	$\dot{C}_{W_{Pump}}/\dot{W}_{Pump} = \dot{C}_{W_{T2}}/\dot{W}_{T2}$, $\dot{C}_{10a} = (1 - x_3)\dot{C}_{10}$
FT1		$\dot{C}_{21} = (1 - x_4)\dot{C}_{16}$
EV1		$\dot{C}_{18}/\dot{E}_{18} = \dot{C}_{17}/\dot{E}_{17}$ $\dot{C}_{17} = x_4\dot{C}_{16}$
FT2		$\dot{C}_{19} = (1 - x_5)\dot{C}_{18}$
EV2		$\dot{C}_{24}/\dot{E}_{24} = \dot{C}_{25}/\dot{E}_{25}$ $\dot{C}_{24} = x_5\dot{C}_{18}$

Ejector	$\dot{C}_{16} = \dot{C}_{10b} + \dot{C}_{19} + \dot{Z}_{Ejector}$	$\dot{C}_{10b} = x_3\dot{C}_{10}$
Evaporator	$\dot{C}_{26} + \dot{C}_{06} = \dot{C}_{25} + \dot{C}_{05} + \dot{Z}_{Evap.}$	$\dot{C}_{26}/\dot{E}_{26} = \dot{C}_{25}/\dot{E}_{25}$, $\dot{C}_{05} = 0$
C2	$\dot{C}_{23} = \dot{C}_{28} + \dot{C}_{W_{C2}} + \dot{Z}_{C2}$	$\dot{C}_{W_{C2}}/\dot{W}_{C2} = \dot{C}_{W_{T1}}/\dot{W}_{T1}$
Mixer2	$\dot{C}_{28} = \dot{C}_{27} + \dot{C}_{22}$	
C3	$\dot{C}_{27} = \dot{C}_{26} + \dot{C}_{W_{C3}} + \dot{Z}_{C3}$	$\dot{C}_{W_{C3}}/\dot{W}_{C3} = \dot{C}_{W_{C2}}/\dot{W}_{C2}$

Table 3: Equations for fuel and product exergy of each component in STC-EI [52]

Components	**Fuel Exergy**	**Product Exergy**
WHE1	$\dot{E}_{g1} - \dot{E}_{g2}$	$\dot{E}_5 - \dot{E}_4$
Turbine1	$\dot{E}_5 - \dot{E}_6$	$\dot{W}_{T1}$
HTR	$\dot{E}_6 - \dot{E}_7$	$\dot{E}_4 - \dot{E}_3$
LTR	$\dot{E}_8 - \dot{E}_9$	$\dot{E}_3 - \dot{E}_2$
C1	$\dot{W}_C$	$\dot{E}_2 - \dot{E}_{1a}$
Cooler1	$\dot{E}_9 - \dot{E}_1$	$\dot{E}_{02} - \dot{E}_{01}$
Cooler2	$\dot{E}_{29} - \dot{E}_{10}$	$\dot{E}_{04} - \dot{E}_{03}$
WHE2	$\dot{E}_{g2} - \dot{E}_{g3}$	$\dot{E}_{12} - \dot{E}_{11}$
Turbine2	$\dot{E}_{12} - \dot{E}_{13}$	$\dot{W}_{T2}$
Mixer1	$\dot{E}_7 + \dot{E}_{13} + \dot{E}_{23}$	$\dot{E}_8$
SLHX	$\dot{E}_{1b} - \dot{E}_{29}$	$\dot{E}_{22} - \dot{E}_{21}$
Pump	$\dot{W}_{Pump}$	$\dot{E}_{11} - \dot{E}_{10a}$
EV1	$\dot{E}_{17}$	$\dot{E}_{18}$
EV2	$\dot{E}_{24}$	$\dot{E}_{25}$

Ejector	$\dot{E}_{10b} + \dot{E}_{19}$	$\dot{E}_{16}$
Evaporator	$\dot{E}_{25} - \dot{E}_{26}$	$\dot{E}_{06} - \dot{E}_{05}$
C2	$\dot{W}_{C2}$	$\dot{E}_{23} - \dot{E}_{28}$
Mixer2	$\dot{E}_{27} + \dot{E}_{22}$	$\dot{E}_{28}$
C3	$\dot{W}_{C3}$	$\dot{E}_{27} - \dot{E}_{26}$

Table 4: Exergoeconomic performance evaluation parameters [60]

Items	Functions
Average cost per unit exergy of fuel	$c_{F,k} = \dot{C}_{F,k}/\dot{E}_{F,k}$
Average cost per unit exergy of product	$c_{P,k} = \dot{C}_{P,k}/\dot{E}_{P,k}$
Cost rate of exergy destruction	$\dot{C}_{D,k} = c_{F,k}\dot{E}_{D,k}$
Relative cost difference	$r_k = (c_{P,k} - c_{F,k})/c_{F,k}$
Exergoeconomic factor	$f_k = \dot{Z}_k/(\dot{Z}_k + \dot{C}_{D,k})$

4.5 System Flowchart and Analysis Chronology

Mathematical models for the systems are built and solved in Python using the CoolProp library. The ranges and values for input parameters were selected from previous literature by Zhang et al. [29] which conducted extensive analysis on the impact of the mentioned input parameters in the power cycle. The flowchart in **Figure 4** indicates four different routes for the steps followed in solving four STCs. For convenience some of the state points have been represented as variables like: i, j and k. Here, i indicates the evaporator inlet state, j indicates C2 exit state and k stands for Cooler2 exit state. Since the state no. for these states vary between STCs they have been provided in a box at upper-right of the flow chart alongside the color code followed for individual STCs. Certain state points and values were solved using a relaxation method with suitable weights. In the flow start to step 4 and step 11 to end are all same for the systems. The equations to be solved only diverges in between. In solving some of the properties including entrainment ratio, w for STC-EI and STC-EE, LTR cold side exit temperature, T_3 and cooler2 exit temperature, T_k , a relaxation method was adopted in conjunction with the equations. These are indicated by the loops in the flowchart. The loop for T_3 and T_k is common for all the cycle. But STC-EE and STC-EI requires an extra loop to be solved for entrainment ratio, given the presence of ejector in these cycles.

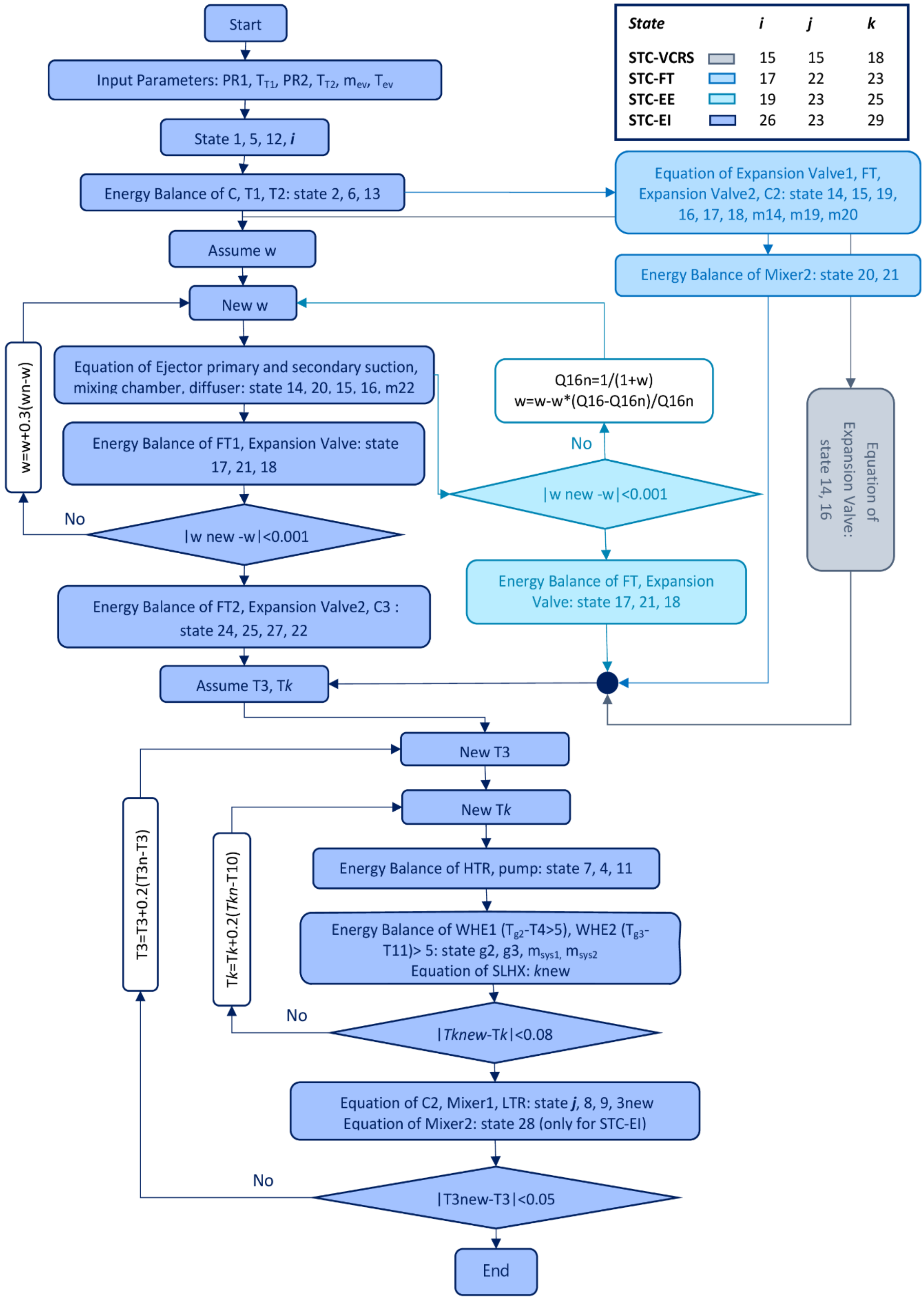

Figure 4: Flowchart for thermodynamic simulation of: STC-VCRS, STC-FT, STC-EE and STC-EI

4.6 Model Validation

The models of the component systems that make up the four combined cycle systems has been compared to and validated against previous studies. The common topping power cycle regenerative sCO_2 – tCO_2 has been validated against the works of Zhang et al. [29] and compared in **Table 5**. The reference study was conducted by developing mathematical models using properties available in REFPROP library in MATLAB software. The validation is done using properties from the CoolProp library in Python. The comparison has been done for the optimum operating condition for regenerative sCO_2 – tCO_2 cycle. There exists a negligible difference between our study and the work of Zhang et al. [29] due to the use of different software for simulation, as shown in **Figure 5**.

Table 5: Validation for sCO_2-tCO_2 cycle

Parameters	Zhang et al. (Cycle 3)	Present study	Difference (%)
W_{net} (MW)	518.798	519.077	0.054
η_{ex} (%)	65.442	65.407	0.053
$\eta_{ex,sys1}$ (%)	73.573	73.623	0.068
$\eta_{ex,sys2}$ (%)	43.228	43.178	0.115
c_{total} (\$/GJ)	7.609		

PR1=3.5, PR2=3.5, T_{T1}=445, T_{T2}=245, η_{T1}=0.90, η_{T2}=0.85, η_C=0.85, η_{pump}=0.80, ε_{HTR}=0.86, ε_{LTR}=0.86

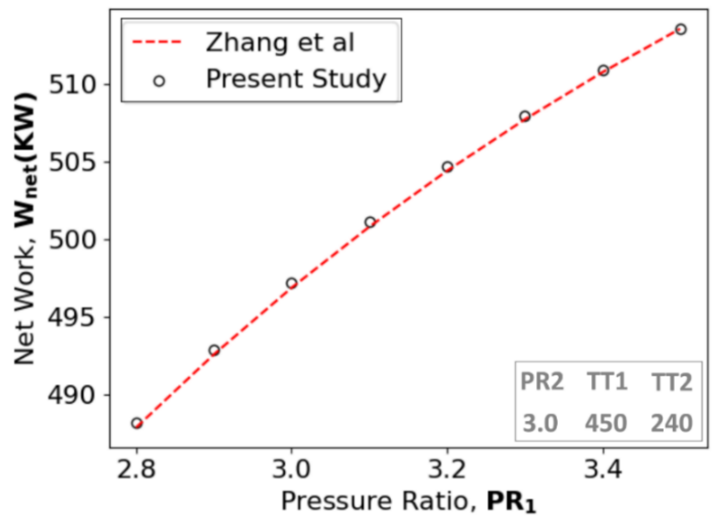

Figure 5: Comparison of Present study with the study on sCO_2-tCO_2 cycle (Cycle3) by Zhang et al. [29]

Experimental validation has been conducted for VCRS and VCRS with SLHX using the data found in the works of Babiloni et al. [52]. **Table 7** contains the comparison between Q_R and COP of experimental data and present study. The maximum deviation seen in **Table 7** is 4.11% for SLHX and 1.42% for VCRS which is well below the acceptable limit. Additionally, a graphical comparison of the same provided in **Figure 7** shows similar trends for experimental data and present study.

In order to consolidate the validity of the numerical model for the ejector enhanced bottoming refrigeration system, a model for standalone ejector enhanced VCRS is developed, and it is compared against the work of Li et al. [66]. The impact of pressure drop on COP between the two models were compared. COP was evaluated under the conditions of, $T_{evp} = 5^{o}$ C, $T_{cond} = 5^{o}$ C, $\eta_n = \eta_m = 0.85, \eta_d = 0.95$. The results obtained through the numerical model closely resembeles the findings in the work, as seen from **Figure 6** This is sufficient evidence confirming the reliability of the model.

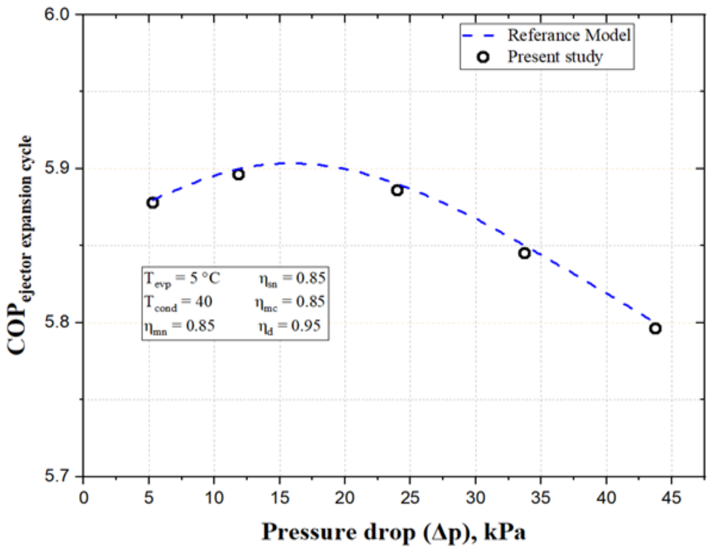

Figure 6: Validation of Ejector enhanced VCR model against the work of Li et al. [66]

Table 6 depicts the variation in COP due to changes in T_{evp} for FT enhanced VCRS found in works of Qi et al. [67] under the following operating conditions: T_{cond}= 50ºC, $\Delta T_{subcool}$ = 5ºC, $\eta_{is} = 0.75$, refrigerant mass flow rate, m_{ev}=1 kg/s. The COP of the developed model was obtained for the same set of T_{evp} and compared. **Table 6** also shows slight deviation in between the present study and COP obtained by Qi et al. [67] due to a variation in database used to emulate the models. Present work used CoolProp library to obtain the data whereas the NIST database was used to obtain data for the literature. However, the deviation is within limit, therefore, the reliability of the FT enhanced VCRS model can also be confirmed.

Table 6: Validation of FT enhanced VCRS model with Qi et al. [67]

T_{evap} (ºC)	COP (Present Work)	COP (Qi et al.)	Relative Difference (%)
-30	2.7167	2.707	0.35833
-25	2.9057	2.8973	0.289925
-20	3.1242	3.0982	0.839197

-15	3.3797	3.3418	1.134119
-10	3.6823	3.6066	2.09893
-5	4.0463	3.9515	2.399089
0	4.492	4.3578	3.079536

Table 7: Validation of VCRS and SLHX system through experimental data provided by Babiloni et al. [68]

T_{evap} (°C)	Cooling Load, Q_R of Experimental Setup (KJ/kg)	Cooling Load, Q_R of Current Study (KJ/kg)	Percent Error (%)	COP of Experimental Setup	COP of Current Study	Percent Error (%)
			VCRS			
-15	146.39	145.63	0.519	1.61	1.63	1.422
-10	149.38	148.86	0.348	2.23	2.25	0.976
-5	152.49	152.06	0.285	3.02	3.05	0.855
			SLHX			
-15	160.82	159.75	0.669	1.56	1.62	4.114
-10	162.17	161.52	0.404	2.25	2.33	3.356
-5	163.52	163.21	0.193	3.01	3.08	2.303

$T_{cond} = 40^o$ C, $\Delta T_{subcool} = 2.4^o$ C, $\Delta T_{subcool} = 10.6^o$ C

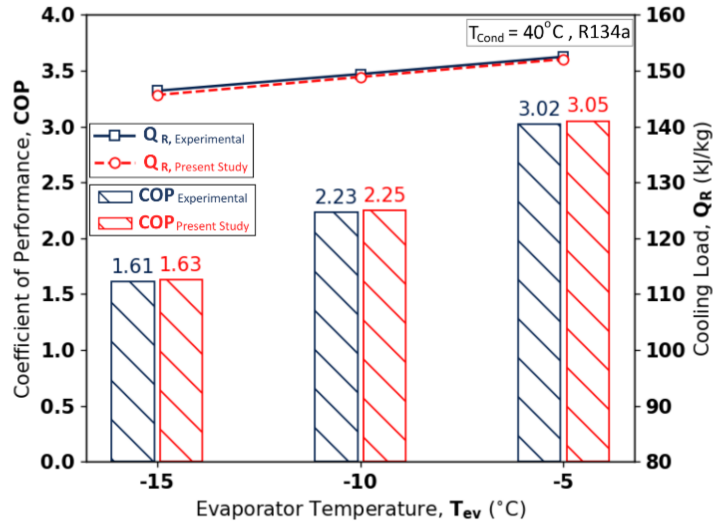

(a)

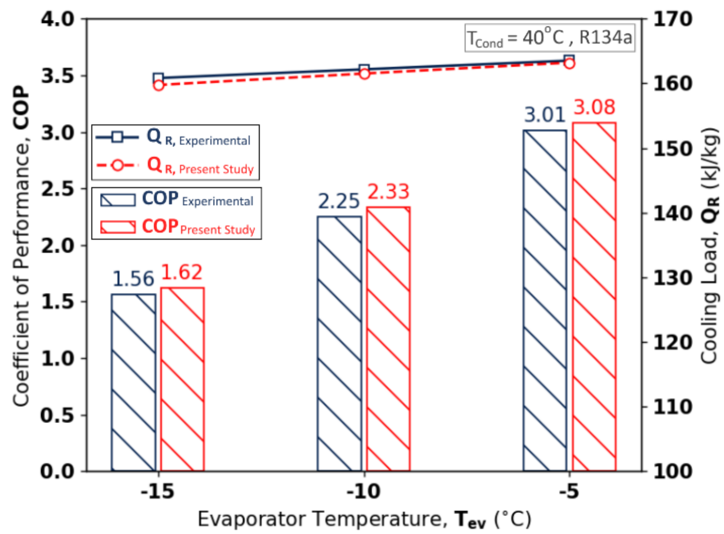

(b)

Figure 7: Validation of (a) VCRS and (b) SLHX system through experimental data provided by Nabil et al. [64]

5. Results and Discussions

The aim of this research is to model a WHR cycle with combined cooling and power, to obtain high net output in terms of either power or cooling. Additionally, the study aims to reduce the cost per unit output, c_{total} as much as possible. Moreover, comparison between four different system configuration with varying refrigeration system has been conducted. **Table 8** contains the information regarding the properties of the ICE exhaust gas chosen as the heat source for this study. **Table 10** presents the properties at different states in STC-EI system under a specific operating condition displayed in **Table 9**.

Table 8: Engine and exhaust gas parameters

Parameters	Values	Exhaust gas molecules	Values (%)
Net power output (kW)	2928	CO_2	9.1
Fuel Consumption (kW)	7002	H_2O	7.4
Electrical efficiency (%)	41.8	N_2	74.2
Engine speed (rpm)	1000	O_2	9.3
Exhaust temperature (°C)	470	-	-
Exhaust mass flow (kg/h)	15,673	-	-

Table 9: Input Parameters for thermodynamic simulation [29],[69]

Parameters	Values
T_0 (° C)	25

P_0 (MPa)	0.101325
T_1 (^{o} C)	32
P_1 (MPa)	7.6
T_{T1}	450
PR_1	3.0
T_{T2} (^{o} C)	240
PR_2	2.2
η_{T1}	0.90
$\eta_{MC\&RC\&C}$	0.85
η_{T2}	0.85
η_{Pump}	0.80
$\varepsilon_{HTR\&LTR\&Recuperator}$	0.86
$\Delta T_{WHE1, end}$ (^{o} C)	10
$\Delta T_{WHE2, end}$ (^{o} C)	≥ 5
$\Delta T_{Cooler2, end}$ (^{o} C)	5
T_{ev} (^{o} C)	-15
m_{ev} (Kg/s)	0.4
Ejector	
η_n	0.85
η_d	0.85
η_m	0.95
ΔP (MPa)	0.2

Table 10: Properties at different state points for STC-EI.

State Points	P (MPa)	T (^{o} C)	h (kJ/kg)	s (kJ/ (kg-K))	m (kg/s)	Q	$\dot{C}$ ($/h)	c ($/GJ)
1	7.600	32.00	315.08	1.376	7.06	-	89.95	16.46
2	22.800	70.31	342.47	1.388	4.23	-	61.91	17.02
3	22.800	144.92	502.71	1.812	4.23	-	76.11	18.34
4	22.800	268.39	681.72	2.190	4.23	-	97.71	18.93
5	22.800	450.00	908.97	2.552	4.23	-	114.8	16.45
6	7.600	329.30	786.89	2.575	4.23	-	82.5	16.45
7	7.600	170.74	607.87	2.230	4.23	-	63.41	16.45
8	7.600	160.15	595.70	2.202	7.06	-	104.3	16.46
9	7.600	82.89	499.71	1.957	7.06	-	94.65	16.46
10	7.600	30.00	289.61	1.292	2.83	-	35.95	16.46
11	16.720	49.19	305.53	1.302	2.15	-	30.05	17.07
12	16.720	240.00	659.99	2.203	2.15	-	38.4	15.84
13	7.600	168.80	605.66	2.225	2.15	-	30.94	15.84
14	3.282	-2.26	280.52	1.298	0.68	0.36	-	-
15	3.282	-2.26	295.50	1.353	0.75	0.42	-	-
16	4.893	13.39	303.24	1.357	0.75	0.37	9.662	17.15
17	4.893	13.39	235.26	1.120	0.47	0.00	6.08	16.92
18	3.482	-0.04	235.26	1.129	0.47	0.15	6.004	16.92

19	3.482	-0.04	430.92	1.846	0.07	1.00	0.9159	18.44
20	3.282	-2.26	429.12	1.847	0.07	0.99	-	-
21	4.893	13.39	418.87	1.761	0.28	1.00	3.581	17.57
22	4.893	29.39	452.30	1.875	0.28	-	3.72	18.29
23	7.600	74.97	488.13	1.925	0.68	-	9.922	18.12
24	3.482	-0.04	199.91	1.000	0.40	0.00	5.088	16.67
25	2.291	-15.00	199.91	1.008	0.40	0.13	5.028	16.67
26	2.291	-15.00	436.27	1.924	0.40	1.00	4.149	16.67
27	4.893	42.95	472.80	1.941	0.40	-	5.129	17.44
28	4.893	37.12	464.40	1.914	0.68	-	8.849	17.8
29	7.600	31.89	311.80	1.365	2.83	-	36.02	16.46
g1	0.101	470.00	987.60	7.447	4.35	-	-	-
g2	0.101	278.39	766.76	7.104	4.35	-	-	-
g3	0.101	120.50	591.70	6.731	4.35	-	-	-

5.1 Parametric Analysis

The parameters selected for analysis and optimization are: pressure ratio of HTPC (PR_1), turbine inlet temperature of HTPC (T_{T1}), pressure ratio of LTPC (PR_2), turbine inlet temperature of LTPC (T_{T2}), evaporator mass flow rate (m_{ev}) and evaporator inlet temperature (T_{ev}). Since, T_{T1} and PR_1 defines the greatest pressure and temperature of the systems, their effect on performance is significant. Similarly, T_{T2} and PR_2 has an impact on the performance of LTPC. So, these four parameters have been analyzed for the power cycles. Moreover, m_{ev} and T_{ev} are significant in controlling the performance of the refrigeration system. Therefore, the parametric analysis of these two parameters has also been performed.

5.1.1 Effect of HTPC Pressure Ratio (PR1)

From **Figure 8(b)** it is evident, COP remains constant for all four cycles even though PR1 increases. This is because, the cooling load Q_R as well as the work done by compressor 3, W_{c3} in refrigeration cycles remain unaffected by any variation in PR1. **Figure 8(b)** also shows, increasing PR1 increases UF. Since, cooling load remains unchanged this is solely due to an increase in net work output, W_{net}. Raising PR1 increases the enthalpy difference across turbine 1 inlet and exit (h_5-h_6) which increases W_{T1}. PR1 also increases work done by power cycle compressor, W_c. However, the increase in W_{T1} is greater resulting in an effective increase in W_{net}. On average, STC-EI has the highest COP (3.011) owing to its high cooling Q_R and low W_{c3}. STC-VCRS has the lowest Q_R for almost the same W_{c3} and thus the lowest COP (1.847). STC-FT has a higher COP than STC-EE since under the given condition it has both a lower W_{c3} and a higher Q_R than STC-EE.

Increasing thermal efficiency η_{th} in **Figure 8(a)** is further testament to the rise in W_{net} with PR1. Since Q_R impacts η_{ex} much less than W_{net}, η_{ex} also increases alongside PR1. The η_{th} for all the cycles are quite similar. STC-EE, however, has a lower η_{th} due to increased W_{c3}. The mass flow rate across the compressor in STC-EE is higher than the flow across the compressor in STC-VCRS as well as either of the compressors for STC-FT and STC-EI owing to entrainment.

For constant T_{T1} higher PR_1 decreases the turbine outlet temperature T_6. As a result, HTR hot side inlet temperature increases, so does HTR cold side exit temperature T_4. Temperature difference of CO_2 across WHE1, ΔT_{WHE1} is thus increased and WHE1 inlet mass m_4 decreased. The` decreased mass flow rate contributes to diminishing cost for LTR, HTR, T1 and C1. Cost must also decrease due to increase in W_{net}. The trend of c_{total} reduction with PR_1 is seen in **Figure 8(c)**.

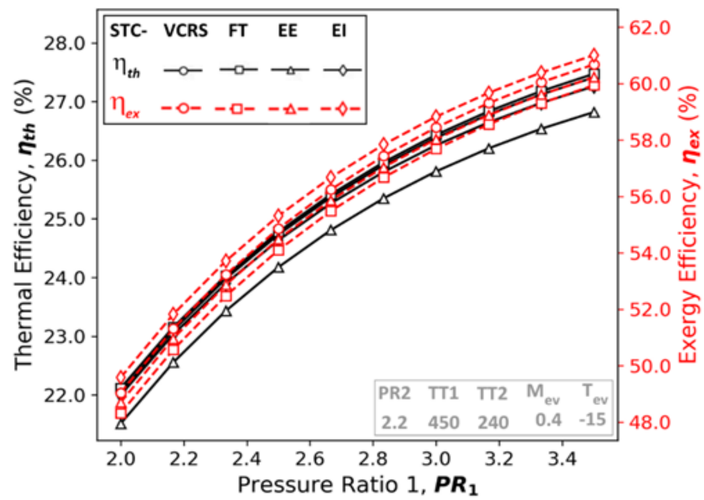

(a)

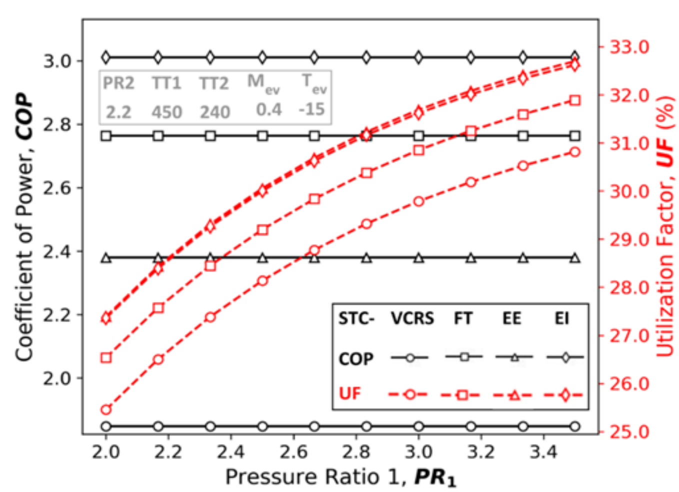

(b)

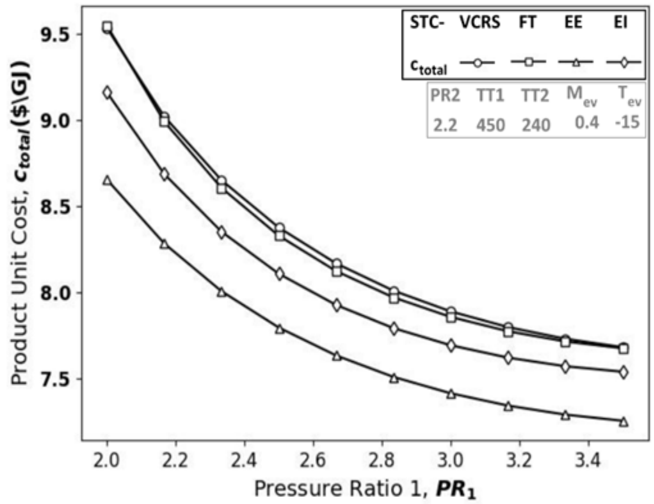

(c)

Figure 8: Effect of HTPC Pressure Ratio (PR1) variation on the cycle (a) η_{th} and η_{ex} (b)COP and UF (c)c_{total}

5.1.2 Effect of LTPC Pressure Ratio (PR2)

Raising PR2 raises UF as per **Figure 9(b)**. Higher pressure difference means higher expansion of fluid across turbine, which must produce more work. Therefore, raising PR2 under constant turbine 2 inlet temperature, TT2 increases the work done by turbine, W_{T2} just like in case of PR1. This positively affects UF and COP remains unaffected by PR2. Growing W_{T2} also increases η_{th} and η_{ex} in **Figure 9(a)**.

Figure 9(b) illustrates the variation of c_{total} in the cycles with PR_2. Initially increasing PR_2 results in a decrease in c_{total}. But after reaching a minimum the c_{total} starts increasing. As PR_2 increases UF and thus the total product. Increased product decreases cost per unit product, c_{total}. Since the fluid needs to be pumped across a greater pressure difference more work is required. This increases investment, operation and maintenance cost of both pump and turbine. Besides, raising PR_2 at constant T_{T2}, decreases the fluid temperature difference ΔT_{WHE2} across WHE2. Consequently, the mass flow across LTPC increases. The increased mass flow contributes to further increase costs for T2 and pump. Therefore, increased cost eventually manages to overwhelm the cost drop due to $W_{net.}$ Thus, we see a higher cost at high pressure ratios. This however implies, a minimum cost can be obtained for a particular $PR_{2.}$ Additionally, **Figure 9(c)** shows STC-VCRS has the highest c_{total} followed by STC-EE, STC-EI and STC-FT.

A heatmap for UF and contour plot for c_{total} in **Figure 10** presents the interaction between the two pressure ratios in influencing the objectives for STC-VCRS. Similar, interactions are expected in other three cycles. At low HTPC inlet pressure remains unaffected by LTPC pressure changes. The same is true for UF. At high PR_1 we see an optimum PR_2 where the cost is the lowest, then it rises again. PR_2 marginally weighs in on UF at high PR_1. So UF is largest at highest PR_2 and $PR_{1.}$ The c_{total} however, has an optimum $PR_{2.}$

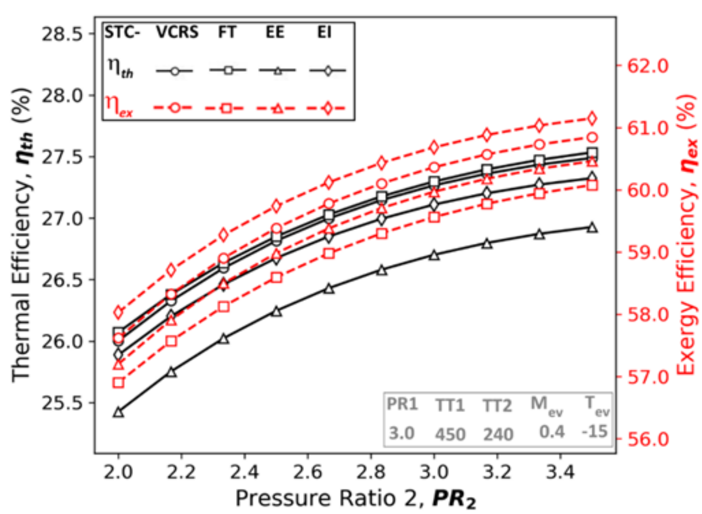

(a)

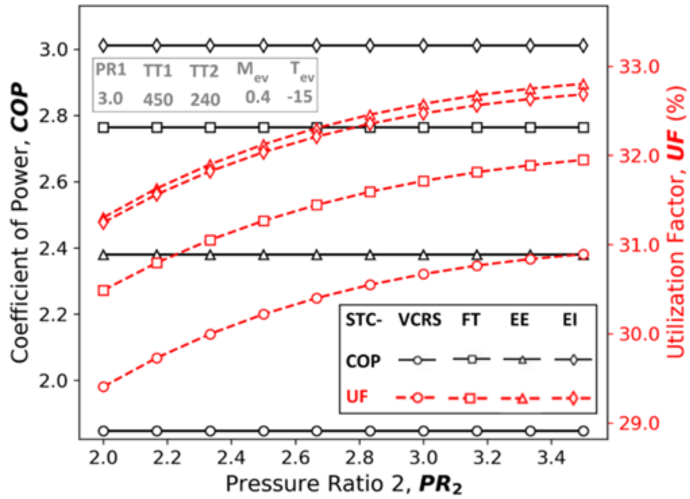

(b)

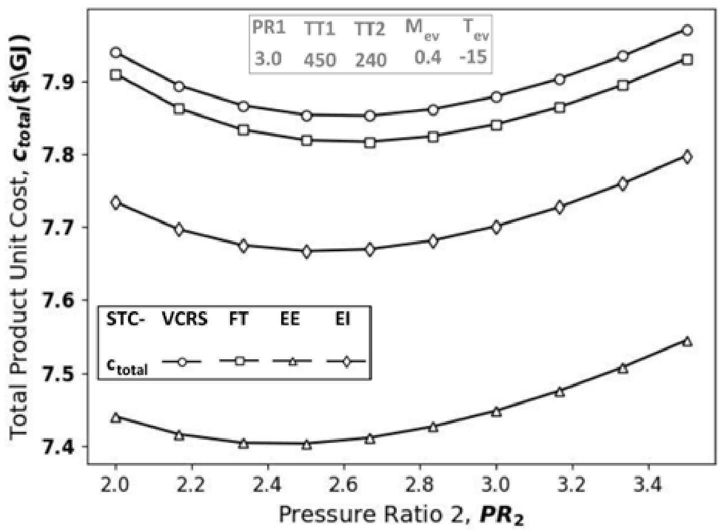

(c)

Figure 9: Effect of LTPC Pressure Ratio (PR2) variation on the cycle (a) η_{th} and η_{ex} (b) COP and UF (c) c_{total}

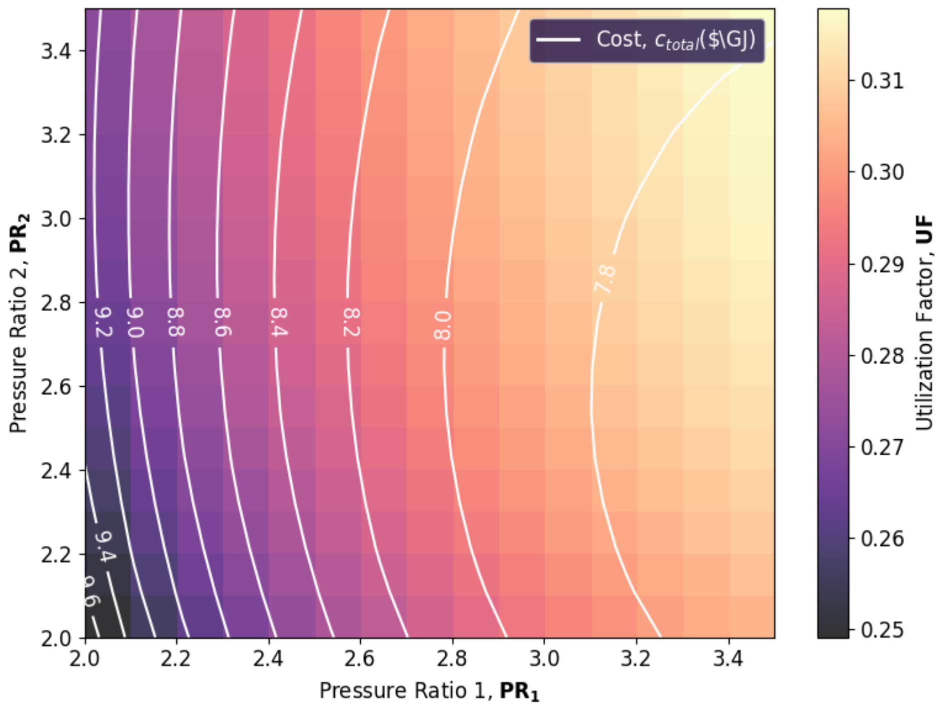

Figure 10: Changes UF and c_{total} for various combinations of Pressure Ratio

5.1.3 Effect of HTPC Turbine Inlet Temperature (T_{T1})

A constant COP proves T_{T1} has no impact on refrigeration section of any of the cycles. UF reduces with increasing T_{T1} in the **Figure 11(b)**. Increasing T_{T1} also increases T4 and thus reduces WHE1 exit temperature, T_{g2}. This limits the heat recovered through WHE1 and reduces the flow rate in HTPC along with the flow across its turbine. The result is a reduction in W_{T1}. Reduced heat exchange in WHE1 also means more heat in WHE2 and thus, more mass flow rate at T2 (m_{12}). As a result, W_{T2} increases. But since W_{T1} makes up the larger portion of W_{net} the effect of its change is dominant. Consequently, there is reduction in W_{net} and therefore in UF. Drop in W_{net} also results in a drop in η_{th} and η_{ex} in **Figure 11(a)**. A positive correlation between T_{T1} and c_{total} is given in

Figure 11(c). Since, W_{net} and c_{total} has an inverse relation, with W_{net} diminishing c_{total} must increase. Thus, minimizing T_{T1} will also minimize c_{total}.

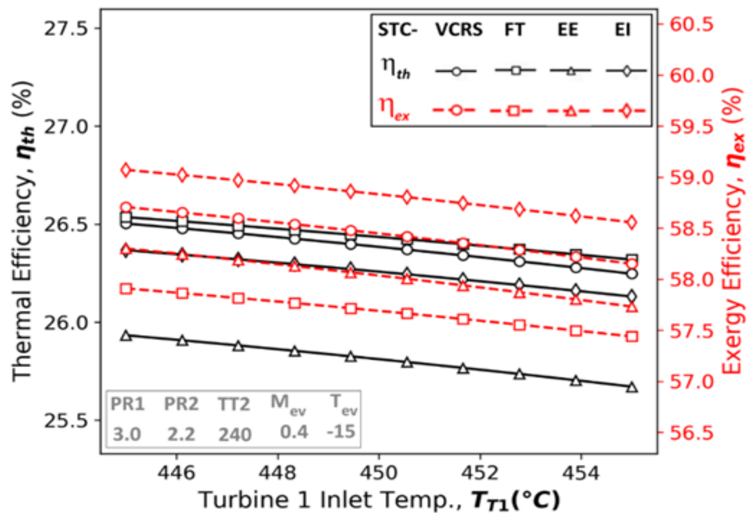

(a)

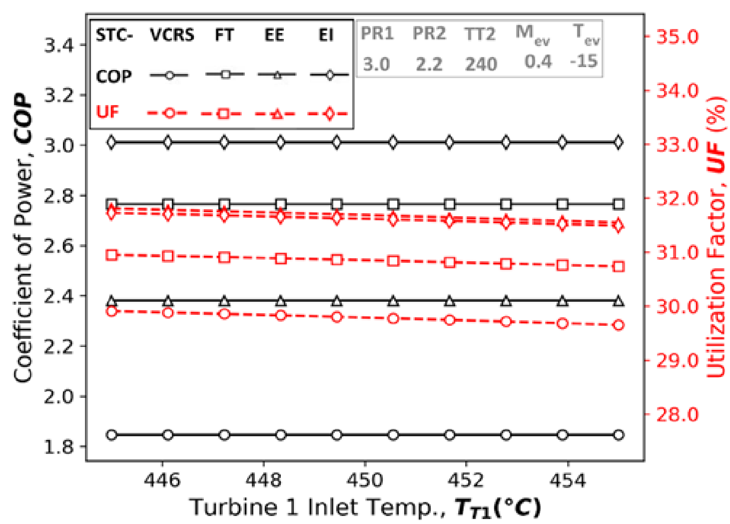

(b)

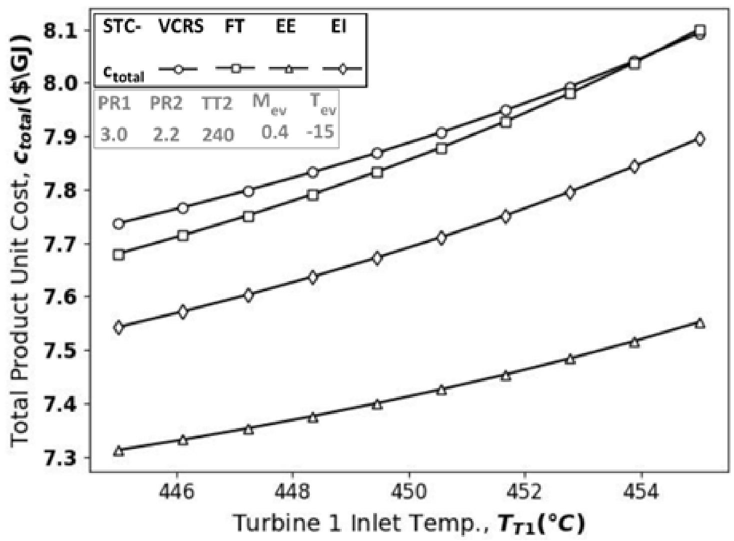

(c)

Figure 11: Effect of HTPC Turbine inlet temperature (T_{T1}) variation on the cycle (a) η_{th} and η_{ex} (b) COP and UF (c) c_{total}

5.1.4 Effect of LTPC Turbine Inlet Temperature (T_{T2})

Increasing T_2 at constant pressure raises outlet temperature, $T_{13.}$ This in turn raises hot side inlet temperature T_8 for LTR and raises cold side exit temperature $T_{4.}$ Since T_{g2} is related to T_4 by a pinch condition it increases as well. As a result, heat transfer in WHE2 increases, and so does mass flow across turbine 2, m_{12}. The consequent rise in W_{T2} is the primary reason for the increase in UF. As usual, the refrigeration cycle remains unaffected by power cycle parameters. Therefore, in **Figure 12(b)** we see no variation in COP with the increase in T_{T2}. In **Figure 12(a)** significant increase in W_{T2} also increases η_{th} and $\eta_{ex.}$ $C_{total.}$ **Figure 12(c)** shows a completely opposite scenario of the previous T_{T1} graph. Here, increasing W_{net} contributes directly to decreasing c_{total}. So, maximizing T_{T2} will minimize $c_{total.}$ From the contours presented on **Figure 13**, T_{T1} has a larger impact on c_{total}

of STC-VCRS than T_{T2} is apparent. The influence of T_{T2} slightly declines as T_{T1} increases. Thus, reducing T_{T1} will more readily help reduce the cost than increasing T_{T2}. The largest UF is found at high T_{T2} and low T_{T1}.

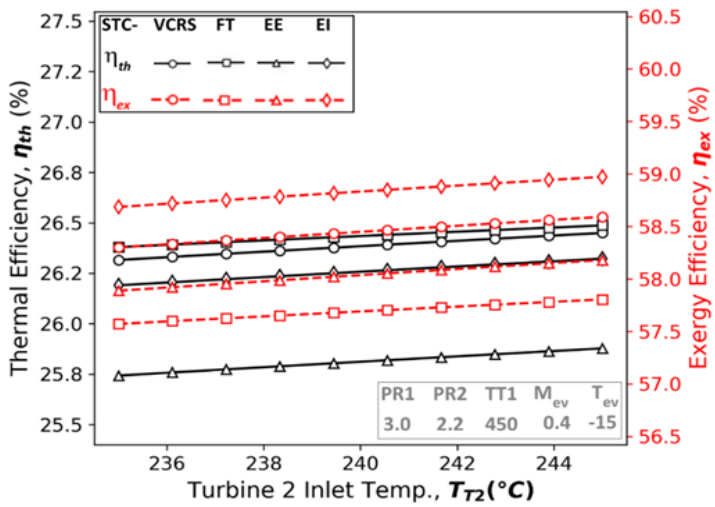

(a)

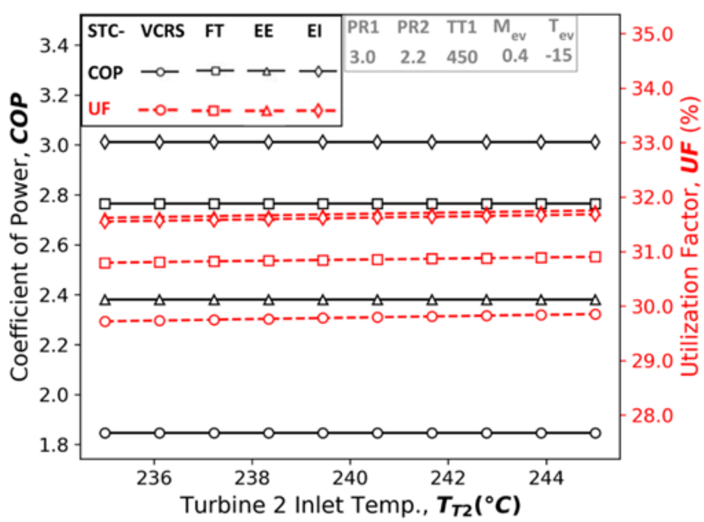

(b)

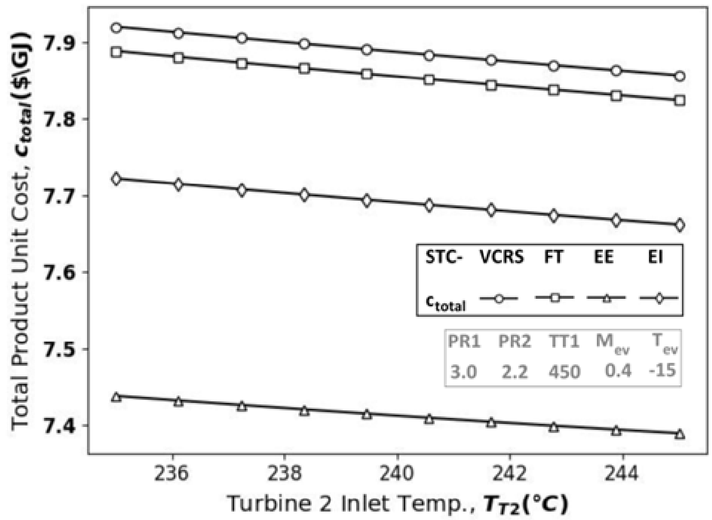

(c)

Figure 12: Effect of LTPC Turbine inlet temperature (T_{T2}) variation on the cycle (a) η_{th} and η_{ex} (b) COP and UF (c) c_{total}

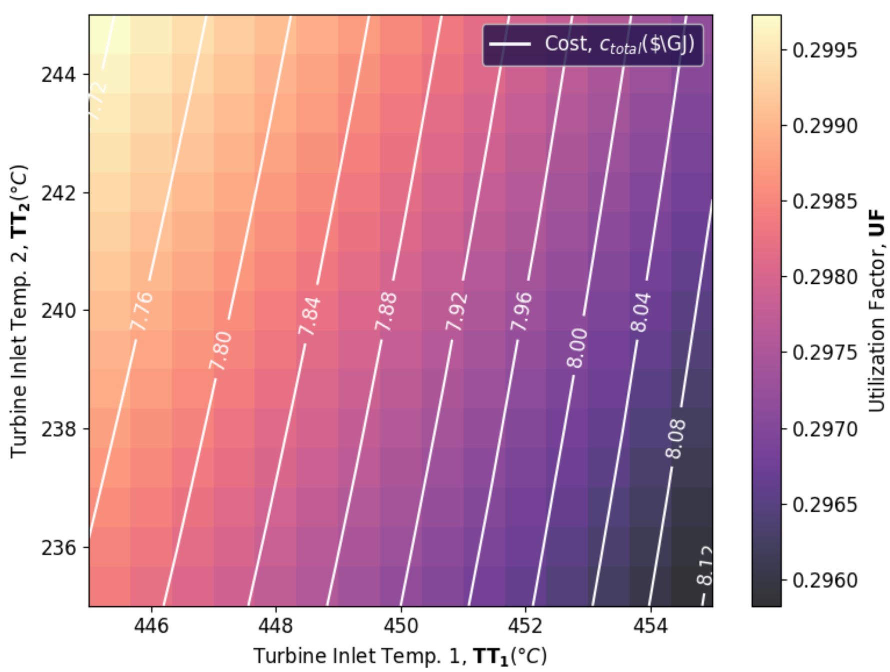

Figure 13: Changes UF and C_{total} for various combinations of Turbine inlet Temperatures

5.1.5 Effect of Evaporator Mass Flow Rate (m_{ev})

Increasing m_{ev} increases the mass flow across compressors in refrigeration cycle, W_{c2} in STC-VCRS and STC-EE and increases W_{c3} alongside W_{c2} in STC-FT and STC-EI. This decreases W_{net} when top cycle outputs remain hardly affected. The decline in W_{net} contributes to the decline in $\eta_{th.}$ Also, as stated before, η_{ex} is affected more severely by changes in W_{net} than that in $Q_{R.}$ This is because η_{ex} directly takes into account E_R which is only a smaller multiple of Q_R. So, η_{ex} is also seen to reduce in the **Figure 14(a)** with increasing m_{ev}. Contrary, to η_{ex}, UF is affected as severely by Q_R as it is by W_{net}. As m_{ev} increases, cooling load is bound to increase. This growth offsets the decline in W_{net}. So, the overall effect is an increase in UF as seen in the **Figure 14(b)**. Though all the cycles show this trend, the steepness varies among them. STC-EE and STC-EI have the steepest increase followed by STC-FT and then STC-VCRS.

Additionally, the **Figure 14(c)** plots variations in c_{total} for the cycles against m_{ev}. The change in c_{total} is the inverse of UF. So, we see a decline with increasing m_{ev}. The decline is least steep for STC-VCRS but becomes increasingly steep for STC-FT, STC-EI and STC-EE. In case of STC-FT the cost soars again after hitting a minimum. Higher m_{ev} besides increasing UF also increases operation cost for the components in the refrigeration cycle. This effect of increased m_{ev} eventually overwhelms that of UF atleast for STC-FT. So, STC-FT has an optimum m_{ev} for which the cost is minimum.

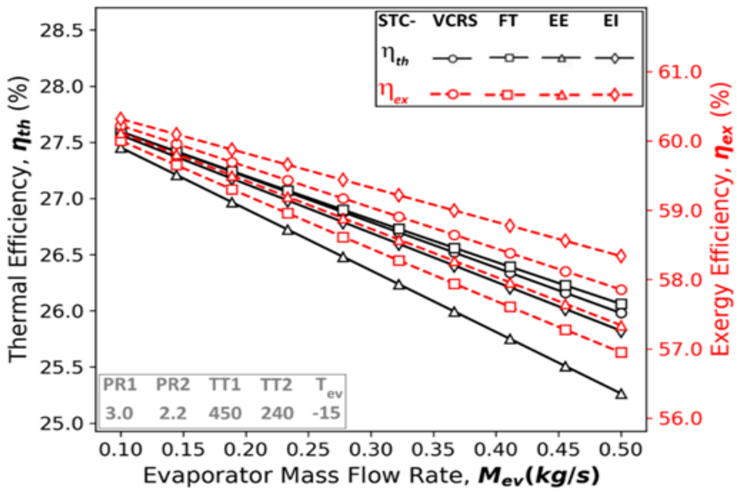
STC- VCRS FT EE EI
η_th
η_ex
PR1 PR2 TT1 TT2 T_ev
3.0 2.2 450 240 -15
Thermal Efficiency, η_th (%)
Exergy Efficiency, η_ex (%)
Evaporator Mass Flow Rate, M_ev(kg/s)
28.5 28.0 27.5 27.0 26.5 26.0 25.5 25.0
61.0 60.0 59.0 58.0 57.0 56.0
0.10 0.15 0.20 0.25 0.30 0.35 0.40 0.45 0.50

(a)

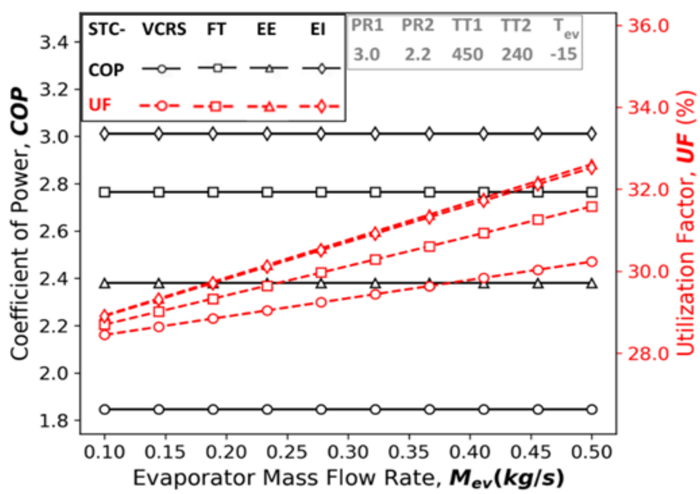
STC- VCRS FT EE EI
COP
UF
PR1 PR2 TT1 TT2 T_ev
3.0 2.2 450 240 -15
Coefficient of Power, COP
Utilization Factor, UF (%)
Evaporator Mass Flow Rate, M_ev(kg/s)
3.4 3.2 3.0 2.8 2.6 2.4 2.2 2.0 1.8
36.0 34.0 32.0 30.0 28.0
0.10 0.15 0.20 0.25 0.30 0.35 0.40 0.45 0.50

(b)

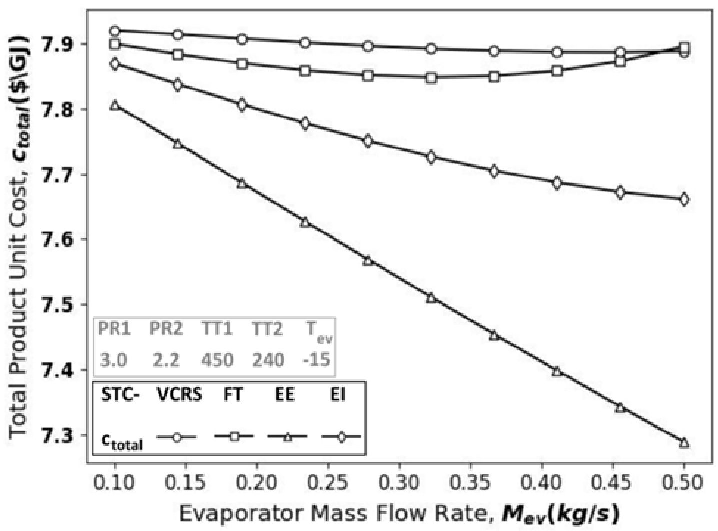

(c)

Figure 14: Effect of evaporator mass flow rate (m_{ev}) variation on the cycle (a) η_{th} and η_{ex} (b) COP and UF (c) c_{total}

5.1.6 Effect of Evaporator Temperature (T_{ev})

In refrigeration cycle increasing T_{ev} decreases the enthalpy of saturated vapor state at evaporator exit. Even though inlet enthalpy slightly decreases as well, it fails to compensate for the loss in exit enthalpy. On the whole enthalpy difference across the evaporator (Δh_{ev}) declines and so does Q_R for constant mass flow rate. On the other hand, compressor has to compress the saturated vapor across a smaller pressure difference owing to the increased T_{ev}. This decreases $W_{c2/c3}$ and increases W_{net}. In the case of η_{th} and η_{ex} where the effect of W_{net} is more prominent we see a rise with increasing T_{ev} in the **Figure 15(a)** The rise in both η_{th} and η_{ex} is much sharper in case of STC-VCRS and STC-EE than in the other to cycle. The effect of declining compressor work is much more direct in these cases due to lack of a flash tank.

It can be seen in **Figure 15(b)**; COP is no longer unaffected unlike in case of the previous parameters. Instead, it rises more sharply as T_{ev} increases. Even though both $W_{c2/c3}$ and Q_R declines, the decline in $W_{c2/c3}$ is more effective as is the case in most refrigeration cycles. In the **Figure 15(b)** for UF we see a decline followed by an initial rise. That is to be expected since W_{net} and Q_R can both affect UF. While initially UF rises due to an increase in $W_{net,}$ the decrease in Q_R has the major impact in the later part. STC-EE and STC-FT hit optimum close to -7.5°C. STC-EI however, appears more stable. But STC-VCRS keeps increasing. The trend for c_{total} seen in **Figure 15(c)** is the opposite of that of UF. Unit cost c_{total} initially falls with rising T_{ev} until a minimum is reached then a rise in c_{total} is seen. The growing net product cuts down the cost. However, as the UF declines, the cost starts growing.

In **Figure 16** we can see, at low m_{ev} and high T_{ev} the impact of m_{ev} on cost is more prominent. That's why the cost lines to the top-left are more vertical. The cost does not vary much with m_{ev} in this region. M_{ev} becomes impactless at high mass flow and medium temperatures, apparent from horizontal lines to the right. Both high m_{ev} and high T_{ev} increases UF. So, both minimum cost and maximum UF can be found when m_{ev} and T_{ev} is high in the case of STC-VCRS.

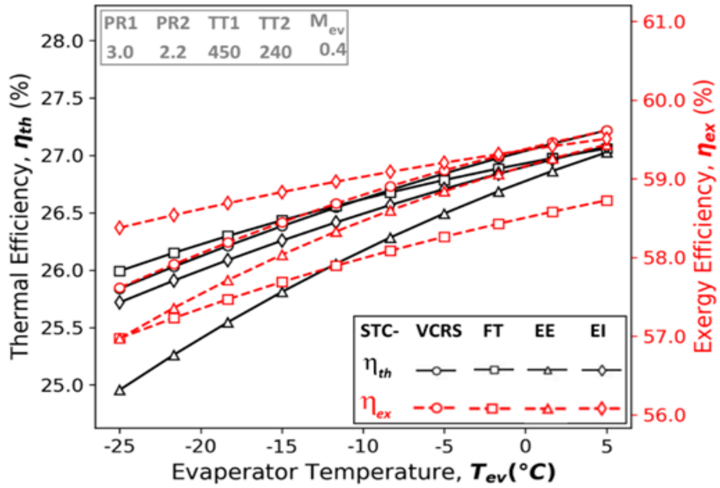

PR1 PR2 TT1 TT2 M_{ev}
3.0 2.2 450 240 0.4
STC- VCRS FT EE EI
η_{th}
η_{ex}
Thermal Efficiency, η_{th} (%)
Exergy Efficiency, η_{ex} (%)
Evaperator Temperature, T_{ev}(°C)

(a)

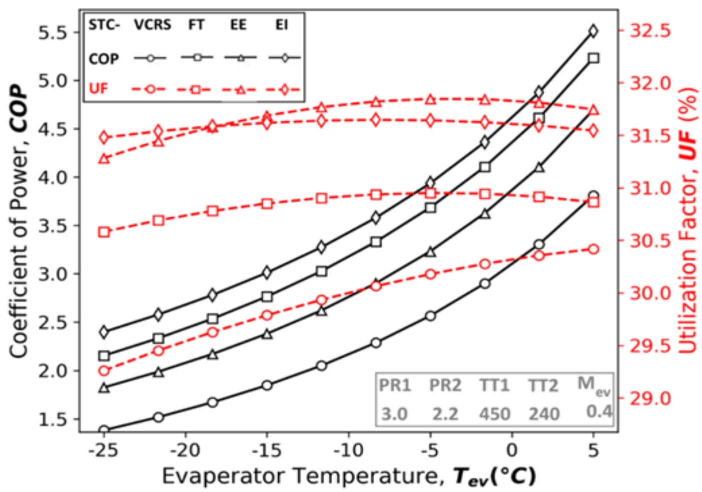

STC- VCRS FT EE EI
COP
UF
PR1 PR2 TT1 TT2 M_{ev}
3.0 2.2 450 240 0.4
Coefficient of Power, COP
Utilization Factor, UF (%)
Evaperator Temperature, T_{ev}(°C)

(b)

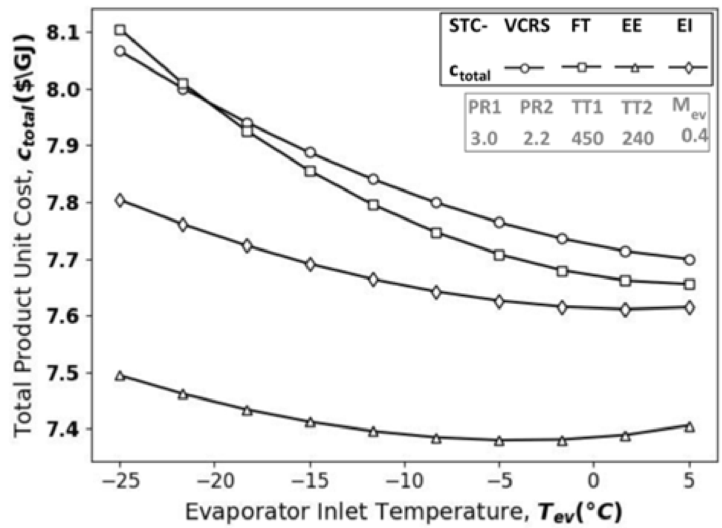

(c)

Figure 15: Effect of evaporator temperature (T_{ev}) variation on the cycle (a) η_{th} and η_{ex} (b) COP and UF (c) c_{total}

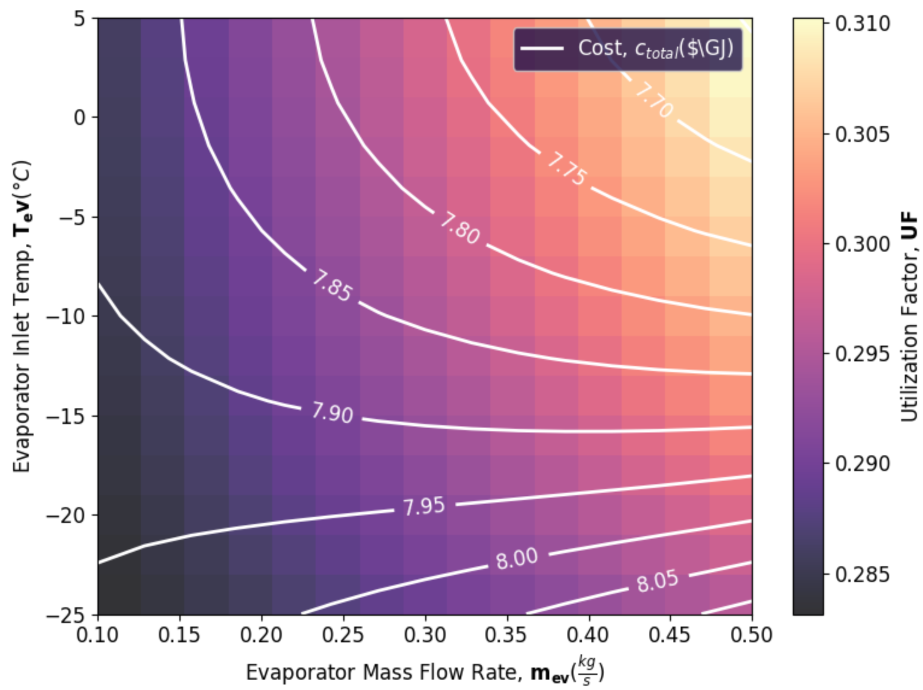

Figure 16: Changes UF and c_{total} for various combinations of Evaporator inlet temp. and mass flow rate

5.2 Exergoeconomic Evaluation

The exergoeconomic results for each component of STC-VCRS, STC-FT, STC-EE and STC-EI have been shown in **Table 11**, **Table 12**, **Table 13,** and **Table 14** respectively. The total cost rate for each component ($\dot{Z}_k + \dot{C}_{D,k}$) accommodates both CIOM cost rate ($\dot{Z}_k$) and exergy destruction cost rate ($\dot{C}_D$) which is a key parameter for exertic cost analysis. Higher value of ($\dot{Z}_k + \dot{C}_{D,k}$) implies that the component should get the maximum importance. Besides the exergoeconomic factor (f_k) denotes the ratio of CIOM cost to the total cost rate. A high value of f_k suggests that a decrease in the investment cost of these components can be achieved at the expense of its component efficiency [60].

For STC-VCRS, the highest $\dot{Z}_k + \dot{C}_{D,k}$ value appears in the Cooler1 (9.22 $/h) followed by the LTR (6.566 $/h) and WHE1 (5.011 $/h). For cooler1, this is due to low exergy value of fluid incoming to it, which results in higher exergoeconomic cost than that of other components. For LTR and WHE1, the significant mass flowrate difference between the hot and cold fluid increases the exergy destruction cost rate. The f_k value for these components are 1.755%, 16.02% and 45.57% respectively which suggests component exergy efficiency of cooler1 and LTR can be improved at the expense of higher CIOM cost. For WHE1, as it is one of the most critical components, has significant CIOM cost with higher exergy destruction cost rate. It needs to be emphasized that here more expense will increase the overall exergy efficiency, therefore efficiency cost trade-off should be weighted before any decision. In the bottom VCRS cycle, Cooler2 with the highest relative cost difference (r_k) of 295.5% has lower f_k value (2.218%) meaning that the irreversibility is very high. This continues to be high for Evaporator (80.32%) and Cooler1

(64.79%) which is because the useful exergy flow is highly limited for these components. The highest f_k value consists in the Turbine1 (51.79%) followed by the Pump (47.82%) which indicates that these components required the largest capital investment. For compressor 1 and compressor 2, f_k values are 24.91% and 14.25%. Choosing a more expensive compressor will help to improve the exergoeconomic performance, which generally means a higher pressure-ratio will be required. The overall exergoeconomic factor of STC-VCRS is 32.66% which means about 67% of the total cost is related to exergy destruction. So, it is a reasonable to pick the components with better performance because the improvement of the exergoeconomic performance would overcome the rise in total investment cost.

For STC-FT, STC-EE and STC-EI, highest $\dot{Z}_k + \dot{C}_{D,k}$ value also belongs to the Cooler1 for the same reason as of STC-VCRS system. In STC-EE and STC-EI, Ejector was introduced which has relatively lower $\dot{Z}_k + \dot{C}_{D,k}$ value (<1 \$/h). This is primarily because Ejector being an expansion device, has similar $\dot{C}_{D,k}$ value of a Expansion valve, which in ideal scenario should be 0. For STC-EE, adding only a Ejector with one flash tank increases irreversibility in SLHX, and therefore $\dot{C}_{D,k}$ is relatively higher than that of other bottom cycles. The r_k values are also consistent with the STC-VCRS for other three systems. For all the cases, Cooler2 has the highest r_k value due to irreversibility. The value becomes maximum for STC-EI which is 448% because of the addition of flash tank which increases the temperature of the inlet stream entering Cooler2. The exergoeconomic factors of sCO_2 turbines (Turbine 1) are all around 50%, indicating that their costs are mostly related to investment costs. Again, the Pump has the second highest f_k value around 47% for other three systems. So, most of the COIM cost are held by Turbine1 and the Pump for all four systems. This suggests, if the requirement is a low costing design, then lowering their thermodynamic performance and exergy efficiency should be the best decision. But in that case, efficiency cost trade-off must be considered before providing any recommendations.

The exergoeconomic impact factor of the total system for STC-FT, STC-EE and STC-EI are 28.86%, 30.14% and 33.03% respectively. This implies that, STC-FT has the most cost associated with exergy destruction. Here, increasing exergy efficiency of the components will inevitably increase the performance of the system. Among all four systems, STC-EI has the highest overall exergoeconomic factor, which is associated with the most expensive components that exhibit relatively higher exergy efficiency. Comparing the exergoeconomic factors of all four systems reveals a scenario of similar behavior with average f_k value of around 30%. Therefore, it is beneficial to choose more expensive components to gain significant performance improvement.

*Table 11***:** *Exergoeconomic results of the STC-VCRS cycle for the base design.*

Components	$\dot{E}_{D,k}$ (KW)	$\dot{C}_{D,k}$ (\$/h)	$c_{F,k}$ (\$/GJ)	$c_{P,k}$ (\$/GJ)	$\dot{Z}_k$ (\$/h)	$\dot{Z}_k + \dot{C}_{D,k}$ (\$/h)	r_k (%)	f_k (%)
Turbine1	28.73	1.68	16.24	17.15	1.805	3.485	5.548	51.79
WHE1	10.99	2.727	68.94	70.47	2.284	5.011	2.218	45.57
WHE2	97.14	1.512	43.25	65.41	0.4238	1.936	51.26	2.726
HTR	36.52	1.84	139.9	158.4	2.534	4.373	13.21	12.1
LTR	25.64	2.255	244.3	283.7	4.301	6.556	16.17	16.02
C1	15.22	1.037	18.94	21.79	0.3442	1.382	15.07	24.91
Cooler1	68.79	7.823	315.9	2363	1.397	9.22	64.79	1.755
Turbine2	14.43	0.8128	15.65	17.53	0.2528	1.066	12.03	23.72
Pump	6.505	0.5109	21.81	26.77	0.4681	0.979	22.72	47.82
C2	3.547	0.2357	18.46	20.78	0.0392	0.2749	12.57	14.25

EV	7.568	0.4403	16.16	16.16	0.0011	0.4414	0.024	0.252
SLHX	1.064	2.7	7047	26776	0.0851	2.785	28	0.314
Evaporator	8.084	4.047	139.1	1256	0.0915	4.139	80.32	2.211
Cooler2	0.699	2.436	9673	38262	0.5524	2.988	295.5	2.218
Total System	324.9	30.06			14.58	44.64		32.66

Table 12: Exergoeconomic results of the STC-FT cycle for base design.

Components	$\dot{E}_{D,k}$ (KW)	$\dot{C}_{D,k}$ ($/h)	$c_{F,k}$ ($/GJ)	$c_{P,k}$ ($/GJ)	$\dot{Z}_k$ ($/h)	$\dot{Z}_k + \dot{C}_{D,k}$ ($/h)	r_k (%)	f_k (%)
Turbine1	28.48	1.727	16.84	17.78	1.79	3.517	5.545	50.89
WHE1	12.29	2.94	66.47	68.02	2.378	5.319	2.342	44.72
WHE2	82.73	1.384	46.46	68.65	0.4448	1.829	47.75	3.114
HTR	52.69	2.469	130.2	154	2.441	4.91	18.33	8.997
LTR	32.82	3.773	319.3	414	3.838	7.611	29.65	9.234
C1	15.12	1.065	19.57	22.52	0.3413	1.406	15.1	24.27
Cooler1	65.23	8.097	344.8	2577	1.405	9.502	64.75	1.706
Turbine2	13.17	0.7689	16.21	18.16	0.2312	1	12.01	23.11
Pump	6.044	0.4898	22.51	27.73	0.4358	0.9256	23.16	47.08
C2	1.682	0.1151	19.01	22.32	0.01075	0.1259	17.41	8.543
EV1	4.612	0.279	16.8	16.8	0.001695	0.2806	0.02217	0.604

SLHX	0.144	4.653	89206	772494	0.1248	4.778	76.6	0.267
Evaporator	12.05	4.354	100.3	906	0.1159	4.47	80.29	2.592
EV2	1.88	0.1113	16.45	16.44	0.00111	0.1124	0.02267	0.987
C3	2.553	0.1743	18.97	21.7	0.01643	0.1907	14.4	8.612
Cooler2	0.887	2.575	8063	32660	0.6138	3.189	305.1	2.328
Total System	332.4	34.97			14.19	49.16		28.86

Table 13: Exergoeconomic results of the STC-EE cycle for the base design.

Components	$\dot{E}_{D,k}$ (KW)	$\dot{C}_{D,k}$ (\$/h)	$c_{F,k}$ (\$/GJ)	$c_{P,k}$ (\$/GJ)	$\dot{Z}_k$ (\$/h)	$\dot{Z}_k + \dot{C}_{D,k}$ (\$/h)	r_k (%)	f_k (%)
Turbine1	28.76	1.764	17.03	17.98	1.806	3.57	5.549	50.59
WHE1	10.88	2.843	72.57	74.17	2.275	5.118	2.208	44.46
WHE2	98.43	1.595	45	68.21	0.4226	2.017	51.56	2.581
HTR	35.21	1.89	149.1	168.2	2.542	4.432	12.8	11.86
LTR	22.89	2.164	262.5	299.3	4.789	6.953	14.01	18.12
C1	15.21	1.083	19.77	22.75	0.3444	1.427	15.05	24.13
Cooler1	71.41	8.663	337	2509	1.437	10.1	64.44	1.632
Turbine2	14.51	0.8563	16.4	18.36	0.2547	1.111	12	22.93
Pump	6.667	0.5434	22.64	27.89	0.471	1.014	23.19	46.43
C2	4.956	0.3433	19.24	21.78	0.04443	0.3877	13.19	11.46

EV	0.389	0.0224	16	16	0.00111	0.02355	0.02271	4.713
SLHX	2.445	6.454	7332	20192	0.126	6.58	17.54	0.194
Evaporator	13.96	4.347	86.51	781.2	0.1263	4.473	80.3	2.824
Ejector	6.076	0.3667	16.77	17.24	0.2686	0.6353	2.85	42.28
Cooler2	0.628	2.87	12689	49063	0.5374	3.407	286.7	1.838
Total System	332.4	35.8			15.45	51.25		30.14

Table 14: Exergoeconomic results of the STC-EI cycle for the base design.

Components	$\dot{E}_{D,k}$ (KW)	$\dot{C}_{D,k}$ ($/h)	$c_{F,k}$ ($/GJ)	$c_{P,k}$ ($/GJ)	$\dot{Z}_k$ ($/h)	$\dot{Z}_k + \dot{C}_{D,k}$ ($/h)	r_k (%)	f_k (%)
Turbine1	28.68	1.698	16.45	17.36	1.8	3.498	5.552	51.45
WHE1	11.37	2.787	68.09	69.62	2.313	5.1	2.254	45.35
WHE2	92.63	1.472	44.14	66.3	0.4289	1.901	50.2	2.832
HTR	41.29	2.032	136.7	156.7	2.504	4.536	14.69	10.97
LTR	19.86	2.033	284.2	323.9	4.583	6.616	13.94	18.4
C1	15.1	1.041	19.15	22.02	0.3433	1.385	14.99	24.79
Cooler1	68.68	8.21	332.1	2506	1.429	9.639	65.46	1.71
Turbine2	14.05	0.801	15.84	17.74	0.2462	1.047	12.03	23.51
Pump	6.277	0.4982	22.05	27	0.4582	0.9565	22.46	47.91
C2	2.08	0.1395	18.63	21.72	0.01596	0.1555	16.6	10.26

EV1	1.251	0.0761	16.92	16.91	0.00131	0.07749	0.02181	1.69
SLHX	0.095	1.611	46745	78765	0.1246	1.735	6.85	0.767
Evaporator	13.03	4.471	95.34	860.8	0.1213	4.592	80.29	2.641
EV2	1.005	0.0603	16.67	16.66	0.00111	0.06142	0.02208	1.807
C3	2.081	0.1387	18.52	21.28	0.01142	0.1502	14.85	7.603
Ejector	2.74	0.1641	16.64	16.93	0.1272	0.2913	1.751	43.66
Cooler2	1.028	2.926	7907	43327	0.3645	3.29	448	1.23
Total System	321.2	30.16			14.87	45.03		33.03

Table 15: Decision Variable Range for optimization

Decision Variables	**Range**
PR_1	2.0 ~ 3.5
T_{T1} (^oC)	445 ~ 455
PR_2	2.0 ~ 3.5
T_{T2} (^oC)	235 ~ 245
m_{ev} (Kg/s)	0.1 ~ 0.5
T_{ev} (^oC)	-25 ~ 5

5.3 Single-objective Optimization

The main output of a power system is $W_{net.}$ A powerplant also requires refrigeration. The main output of a refrigeration system is $Q_{R.}$ Often W_{net} and Q_R have a negative correlation as seen in parametric analysis. The goal is to balance the two and obtain maximum output as measured by UF. However, this must be done at minimum $c_{total.}$ Therefore, maximum UF and minimum c_{total} have been chosen as objectives to be optimized. The six decision variables are PR1, PR2, $T_{T1,}$ $T_{T2,}$ m_{ev} and $T_{ev.}$ The ranges for which the decision variables have been optimized is displayed in **Table 15**. The optimization was conducted using Genetic Algorithm (GA). The results have been presented in **Table 16** and **Table 17**.

As seen in **Table 16**, the UF is maximum for maximum $PR_{1,}$ minimum $T_{T1,}$ maximum $PR_{2,}$ maximum T_{T2} and maximum m_{ev} in all four STCs. However, T_{ev} varies between the systems. Among the four, STC-EI has the highest UF followed by STC-EI, STC-FT and STC-VCRS in order. In terms of exergy, STC-VCRS performs best followed by STC-EI, STC-EE and STC-FT in order. From **Table 17** it is seen c_{total} is maximum for maximum PR_1, T_{T1} and $m_{ev.}$ But $T_{T2,}$ PR_2 and m_{ev} are different for different cycles. STC-FT gives us the lowest c_{total} followed by STC-EI, STC-EE and STC-VCRS in order. PR_2 and T_{ev} vary vastly between the objectives. Clearly, a single operating condition where simultaneously UF is maximum and c_{total} is minimum does not exist.

Table 16: Results of single objective optimization for maximum UF using GA

Items	RSTC	STC-VCRS	STC-FT	STC-EE	STC-EI
PR_1	3.5	3.5	3.5	3.5	3.5
T_{T1} (° C)	445	445	445	445	445
PR_2	3.5	3.5	3.5	3.5	3.5

T_{T2} (° C)	245	245	245	245	245
m_{ev} (Kg/s)	-	0.5	0.5	0.5	0.5
T_{ev} (° C)	-	5	-5.2	-4.8	-9.4
Q_R	0	68.936	100.257	115.079	110.445
Net Output	530.206	570.818	582.977	601.65	596.436
η_{ex}	65.44	63.9	62.2	62.9	63.1
UF	30.761	33.118	33.823	34.906	34.604
COP	-	3.810	3.662	3.254	3.476
c_{total}	7.609	7.506	7.422	7.524	7.413

Table 17: Results of single objective optimization for minimum cost using GA

Items	RSTC	STC-VCRS	STC-FT	STC-EE	STC-EI
PR_1	3.5	3.5	3.5	3.5	3.5
T_{T1} (° C)	445	445	445	445	445
PR_2	2.069	2.51	2.17	2.29	2.24
T_{T2} (° C)	245	245	238.942	245	245
m_{ev} (Kg/s)	-	0.5	0.5	0.5	0.5
T_{ev} (° C)	-	5	-4.6	4.52	1.1
Q_R	0	68.937	99.648	102.419	100.289
Net Output	499.385	561.909	564.714	585.3	580.463
η_{ex}	62.99	62.6	60.0	61.8	61.6

UF	28.97	32.56	32.763	33.958	33.68
COP	-	3.810	3.731	4.603	4.779
c_{total}	7.302	7.330	7.037	7.305	7.159

5.4 Multi-objective Optimization

The optimum performance lies at a high UF and low c_{total}. Non-dominated sorting algorithm (NSGA-II) was used from Pymoo library in Python to search for a series of Pareto front solutions that meet those requirements. From the Pareto fronts displayed on **Figure 17** it is evident that an increase in UF also results in an increase in c_{total}. Therefore, a tradeoff between the two objective exists. A solution with least distance from the origin, the co-ordinate representing highest UF and lowest c_{total} of the front, is chosen as the optimum. The output of the solution for all four STCs has been compared in **Table 18**.

It shows STC-EE has the most energetic performance of the four with STC-EI a close second. STC-EE and STC-EI respectively raise the UF by 16.22% and 15.49% from the base cycle. STC-EE improves upon the UF of STC-VCRS and STC-FT by 4.93% and 3.32% respectively. Moreover, all the proposed systems at their optimum have lower cost than the base RSTC. STC-FT outperforms the proposed systems along with the base system in terms of cost. The unit cost at the optimum operating condition for STC-FT is 4.13% lower than the cost of RSTC. It also shows a 12.36% increase in UF. COP is the largest in STC-EI with a difference of 2.09% and 6.26% from STC-EE and STC-VCRS. STC-FT has the lowest COP. All the advantages, however, come at the cost of reduced exergy. A significant portion of the work is lost in producing refrigeration effect which has a lower exergy value than work.

Table 18: Results of multi-objective optimization for maximum UF and minimum c_{total}

Items	RSTC	STC-VCRS	STC-FT	STC-EE	STC-EI
PR_1	3.5	3.5	3.5	3.5	3.5
T_{T1} (° C)	445	445	445	445	445
PR_2	2.904	3.0	2.935	2.934	3.030
T_{T2} (° C)	243.156	245	239.262	245	245
m_{ev} (Kg/s)	-	0.5	0.5	0.5	0.5
T_{ev} (° C)	-	4.716	-7.345	0.521	-4.349
Q_R	0	69.047	102.378	108.159	105.682
Net Output	514.037	567.532	577.122	596.932	593.264
η_{ex}	64.842	63.4	61.4	62.8	62.9
UF	29.8	32.927	33.483	34.633	34.417
COP	-	3.762	3.429	3.929	4.013
c_{total}	7.435	7.391	7.128	7.369	7.264

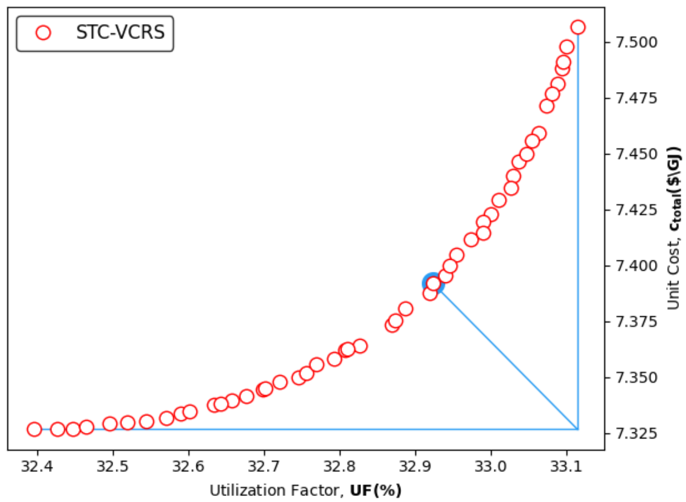
STC-VCRS
Unit Cost, c_{total}($\GJ)
Utilization Factor, UF(%)

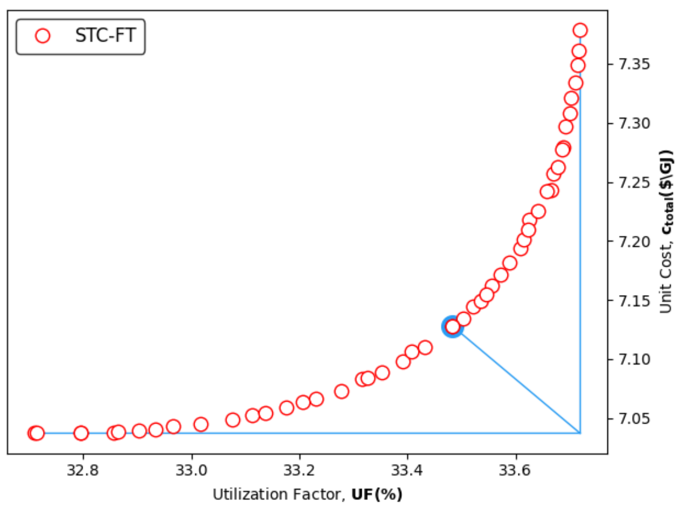
STC-FT
Unit Cost, c_{total}($\GJ)
Utilization Factor, UF(%)

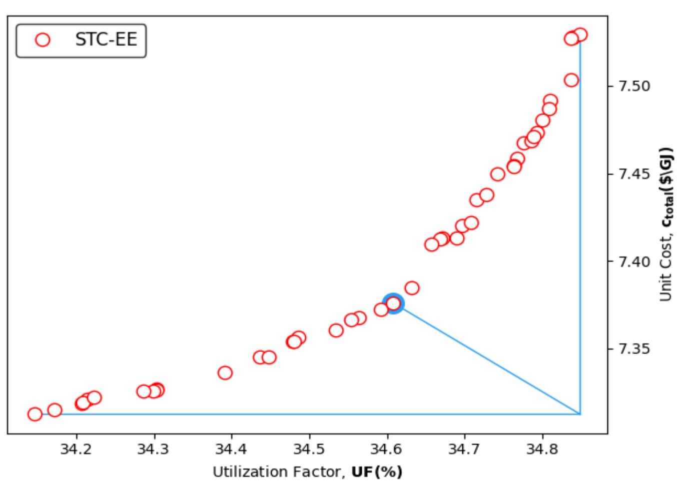
STC-EE
Unit Cost, c_{total}($\GJ)
Utilization Factor, UF(%)

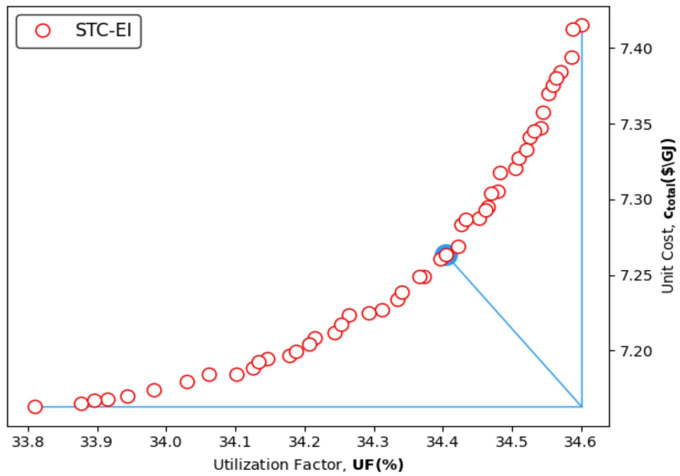

Figure 17: Pareto Fronts obtained after Multi-Objective Optimization

A Sankey diagram for the optimum operating condition of STC-EI is provided in **Figure 18**. The highest exergy destruction, E_D is seen in case Cooler, WHE2 and HTR in order. They are respectively responsible for 27.26%, 16.11% and 15.3% of the total E_D. So, to reduce irreversibility within the cycle performance Cooler1 and WHE2 performance needs to be improved. T_{T2} for the optimum operation of three of the studied systems is the maximum temperature considered for this analysis. This is not the case for RSTC. Attaching the cooling cycles to RSTC has increased T_{g2}. Maximum T_{T2}, 245°C falls behind this significantly. This results in an increased exergy loss in WHE2. The loss may be recovered by increasing maximum T2 inlet temperature. This excludes STC-FT since its T_{T2} is already at optimum. A trigeneration system with combined cooling, heating and power (CCHP) can help recover the exergy loss in cooler.

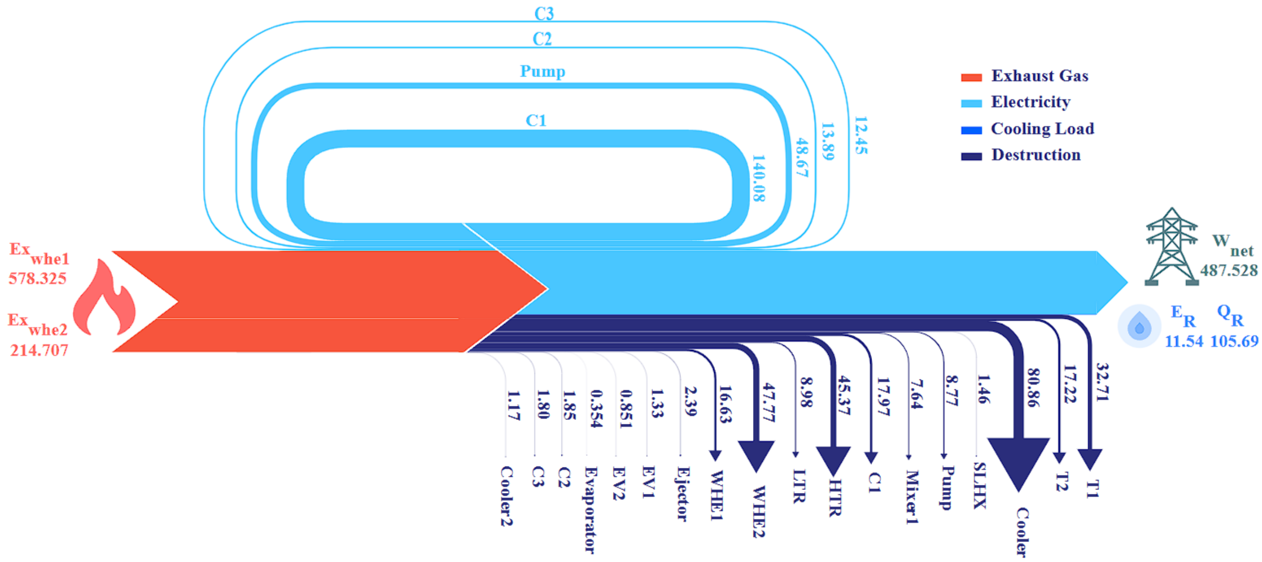

Figure 18: Exergy flow diagram for STC-EI under optimized condition

6. Conclusion

In this study, four novel cogeneration cycles with regenerative sCO_2–tCO_2 are proposed for engine waste heat recovery. The cycles are subjected to energy, exergy, economic and parametric analysis. They are optimized and compared with a reference cycle to find the best layout for cogeneration through waste heat recovery. The following conclusions can be drawn from these:

- High refrigerant mass flow helps improve both thermodynamic and economic performance of cycle. But there is an optimum evaporation temperature that largely varies for each cycle. This can be a deciding factor in determining the application for the proposed layouts.
- A cost improvement is achieved in four cases. Among the four systems STC-FT reduces costs by 4.13% and improves UF by 12.36% optimally. The STC-EI gives 15.29% more UF at 2.3% lower cost than RSTC and 6.26% higher COP than STC-FT. Considering overall performance STC-EI is the best choice for cooling and power production. STC-FT may also be chosen to reduce complexity.
- Ejector vapor injection thus can have considerable advantage over other VCRS as part of fully integrated systems. Cogeneration causes an exergy loss which is an acceptable compromise in high-exergy cycles like RSTC for the considerable cost reduction it can provide. Therefore, STCs are the economic choice for WHR in IC engine powerplants
- Exergy efficiency of the cycle can be improved by reducing exergy destruction at cooler1 and WHE2. This may be done by increasing T_{T2} following further study.

Appendix

The comprehensive mathematical formulations for calculating Z_k of the power cycles examined herein are presented in the **Table A1** that heat exchanger area must be computer in order to calculate its cost. The LMTD method should be used as described in the section 3.3. Besides, the investment cost of the mixing chamber and flash tank is so low to be neglected. It is important to acknowledge that the predicted cost functions shown in **Table A1** were formulated in the year 2019. The transformation formula for calculating cost of present year is, as shown below [29]

$$Cost\ in\ present\ year\ =\ Original\ cost \times \left(\frac{Cost\ index\ for\ present\ year}{Cost\ index\ for\ original\ year}\right) \tag{39}$$

Table A1: Cost functions of the power cycle components [29],[71],[72],[73]

Components	Cost Functions
Turbine	$Z_T = 479.34 \times m_{in} \times [\frac{1}{0.93-\eta_T}] \times \ln(PR_C) \times (1 + e^{(0.036T_{in}-54.4)})$
Compressor	$Z_C = 71.1 \times m_{in} \times [\frac{1}{0.92-\eta_C}] \times PR_C \times \ln(PR_C)$
Pump	$Z_{Pump} = 1120 \times W_{Pump}^{0.8}$
Heat Exchangers	$Z_{HE} = 2681 \times A_k^{0.59}$
Throttling valve	$Z_{TV} = 114.5 \times m_{in}$
Ejector	$Z_{EJ} = 1000 \times 16.14 \times 0.989 \times m_{exit} \times (\frac{T_i}{(0.001 \times P_i)^{0.05}}) \times P_e^{-0.75}$

REFERENCES

[1] R. Zhang, W. Su, X. Lin, N. Zhou, and L. Zhao, "Thermodynamic analysis and parametric optimization of a novel S–CO2 power cycle for the waste heat recovery of internal combustion engines," *Energy*, vol. 209, Oct. 2020, doi: 10.1016/j.energy.2020.118484.

[2] "The Supercritical Thermodynamic Power Cycle," Fergamon Pre~s, 1968.

[3] A. Zhou, X. song Li, X. dong Ren, and C. wei Gu, "Improvement design and analysis of a supercritical CO2/transcritical CO2 combined cycle for offshore gas turbine waste heat recovery," *Energy*, vol. 210, Nov. 2020, doi: 10.1016/j.energy.2020.118562.

[4] J. Sarkar, "Review and future trends of supercritical CO2 Rankine cycle for low-grade heat conversion," Aug. 01, 2015, *Elsevier Ltd*. doi: 10.1016/j.rser.2015.04.039.

[5] L. Zhang, J. J. Klemeš, M. Zeng, and Q. Wang, "Dynamic study of the extraction ratio and interstage pressure ratio distribution in typical layouts of SCO2 Brayton cycle under temperature fluctuations," *Appl Therm Eng*, vol. 212, p. 118553, Jul. 2022, doi: 10.1016/J.APPLTHERMALENG.2022.118553.

[6] S. Mondal and S. De, "CO2 based power cycle with multi-stage compression and intercooling for low temperature waste heat recovery," *Energy*, vol. 90, pp. 1132–1143, Oct. 2015, doi: 10.1016/J.ENERGY.2015.06.060.

[7] K. Braimakis, "Mapping the waste heat recovery potential of CO2 intercooling compression via ORC," *International Journal of Refrigeration*, vol. 159, pp. 309–332, Mar. 2024, doi: 10.1016/J.IJREFRIG.2024.01.008.

[8] B. D. Iverson, T. M. Conboy, J. J. Pasch, and A. M. Kruizenga, "Supercritical CO2 Brayton cycles for solar-thermal energy," *Appl Energy*, vol. 111, pp. 957–970, 2013, doi: 10.1016/j.apenergy.2013.06.020.

[9] F. Correa, R. Barraza, Y. C. Soo Too, R. Vasquez Padilla, and J. M. Cardemil, "Optimized operation of recompression sCO2 Brayton cycle based on adjustable recompression fraction under variable conditions," *Energy*, vol. 227, p. 120334, Jul. 2021, doi: 10.1016/J.ENERGY.2021.120334.

[10] Z. Chang, Y. Zhao, Y. Zhao, G. Liu, Q. Yang, and L. Li, "Off-design performance and control strategies of sCO2 recompression power systems considering compressor operating safety," *Appl Therm Eng*, vol. 232, p. 121044, Sep. 2023, doi: 10.1016/J.APPLTHERMALENG.2023.121044.

[11] G. Angelino, "Carbon Dioxide Condensation Cycles For Power Production," 1968. [Online]. Available: http://www.asme.org/about-asme/terms-of-use

[12] Y. Khan and R. Shyam Mishra, "Thermo-economic analysis of the combined solar based pre-compression supercritical CO2 cycle and organic Rankine cycle using ultra low GWP fluids," *Thermal Science and Engineering Progress*, vol. 23, p. 100925, Jun. 2021, doi: 10.1016/J.TSEP.2021.100925.

[13] Y. Ahn *et al.*, "Review of supercritical CO2 power cycle technology and current status of research and development," Oct. 01, 2015, *Korean Nuclear Society*. doi: 10.1016/j.net.2015.06.009.

[14] K. Wang, Y. L. He, and H. H. Zhu, "Integration between supercritical CO2 Brayton cycles and molten salt solar power towers: A review and a comprehensive comparison of different

cycle layouts," *Appl Energy*, vol. 195, pp. 819–836, 2017, doi: 10.1016/j.apenergy.2017.03.099.

[15] C. F. du Sart, P. Rousseau, and R. Laubscher, "Comparing the partial cooling and recompression cycles for a 50 MWe sCO2 CSP plant using detailed recuperator models," *Renew Energy*, vol. 222, p. 119980, Feb. 2024, doi: 10.1016/J.RENENE.2024.119980.

[16] Y. Khan and R. S. Mishra, "Performance analysis of solar driven combined recompression main compressor intercooling supercritical CO2 cycle and organic Rankine cycle using low GWP fluids," *Energy and Built Environment*, vol. 3, no. 4, pp. 496–507, Oct. 2022, doi: 10.1016/j.enbenv.2021.05.004.

[17] J. Song, X. song Li, X. dong Ren, and C. wei Gu, "Performance improvement of a preheating supercritical CO2 (S-CO2) cycle based system for engine waste heat recovery," *Energy Convers Manag*, vol. 161, pp. 225–233, Apr. 2018, doi: 10.1016/j.enconman.2018.02.009.

[18] F. Meng, E. Wang, B. Zhang, F. Zhang, and C. Zhao, "Thermo-economic analysis of transcritical CO2 power cycle and comparison with Kalina cycle and ORC for a low-temperature heat source," *Energy Convers Manag*, vol. 195, pp. 1295–1308, Sep. 2019, doi: 10.1016/J.ENCONMAN.2019.05.091.

[19] J. Xia, J. Wang, G. Zhang, J. Lou, P. Zhao, and Y. Dai, "Thermo-economic analysis and comparative study of transcritical power cycles using CO2-based mixtures as working fluids," *Appl Therm Eng*, vol. 144, pp. 31–44, Nov. 2018, doi: 10.1016/J.APPLTHERMALENG.2018.08.012.

[20] P. Lisheng, L. Bing, Y. Yuan, S. Weixiu, and W. Xiaolin, “Theoretical investigation on a novel CO2 transcritical power cycle using solar energy,” *Energy Procedia*, vol. 158, pp. 5130–5137, Feb. 2019, doi: 10.1016/J.EGYPRO.2019.01.686.

[21] L. Pan, B. Li, W. Shi, and X. Wei, “Optimization of the self-condensing CO2 transcritical power cycle using solar thermal energy,” *Appl Energy*, vol. 253, p. 113608, Nov. 2019, doi: 10.1016/J.APENERGY.2019.113608.

[22] L. Pan, W. Shi, X. Wei, T. Li, and B. Li, “Experimental verification of the self-condensing CO2 transcritical power cycle,” *Energy*, vol. 198, p. 117335, May 2020, doi: 10.1016/J.ENERGY.2020.117335.

[23] J. Phillips, D. Thimsen, A. Berger, and D. Grace, “EPRI Project Manager.” [Online]. Available: www.epri.com

[24] S. K. Cho, “INVESTIGATION OF THE BOTTOMING CYCLE FOR HIGH EFFICIENCY COMBINED CYCLE GAS TURBINE SYSTEM WITH SUPERCRITICAL CARBON DIOXIDE POWER CYCLE,” 2015. [Online]. Available: http://www.asme.org/about-asme/terms-of-use

[25] M. S. Kim, Y. Ahn, B. Kim, and J. I. Lee, “Study on the supercritical CO2 power cycles for landfill gas firing gas turbine bottoming cycle,” *Energy*, vol. 111, pp. 893–909, Sep. 2016, doi: 10.1016/j.energy.2016.06.014.

[26] G. Manente and F. M. Fortuna, “Supercritical CO2 power cycles for waste heat recovery: A systematic comparison between traditional and novel layouts with dual expansion,” *Energy Convers Manag*, vol. 197, Oct. 2019, doi: 10.1016/j.enconman.2019.111777.

[27] C. Wu *et al.*, "System optimisation and performance analysis of CO2 transcritical power cycle for waste heat recovery," *Energy*, vol. 100, pp. 391–400, Apr. 2016, doi: 10.1016/j.energy.2015.12.001.

[28] S. sen Wang, C. Wu, and J. Li, "Exergoeconomic analysis and optimization of single-pressure single-stage and multi-stage CO2 transcritical power cycles for engine waste heat recovery: A comparative study," *Energy*, vol. 142, pp. 559–577, Jan. 2018, doi: 10.1016/j.energy.2017.10.055.

[29] F. Zhang, B. Chen, G. Liao, and J. E, "Performance assessment and comparative study on novel carbon dioxide based power cycles for the cascade engine waste heat recovery," *Appl Therm Eng*, vol. 214, Sep. 2022, doi: 10.1016/j.applthermaleng.2022.118764.

[30] D. Di Battista, F. Fatigati, R. Carapellucci, and R. Cipollone, "An improvement to waste heat recovery in internal combustion engines via combined technologies," *Energy Convers Manag*, vol. 232, Mar. 2021, doi: 10.1016/j.enconman.2021.113880.

[31] J. Du, J. Guo, Z. Zhang, M. Li, F. Ren, and Y. Liu, "A triple cascade gas turbine waste heat recovery system based on supercritical CO2 Brayton cycle: Thermal analysis and optimization," *Energy Conversion and Management: X*, vol. 16, Dec. 2022, doi: 10.1016/j.ecmx.2022.100297.

[32] A. I. Turja, K. N. Sadat, Y. Khan, and M. M. Ehsan, "Cascading the Transcritical CO2 and Organic Rankine Cycles with Supercritical CO2 Cycles for Waste Heat Recovery," *International Journal of Thermofluids*, vol. 20, p. 100508, Nov. 2023, doi: 10.1016/J.IJFT.2023.100508.

[33] A. I. Turja, K. N. Sadat, M. M. Hasan, Y. Khan, and M. M. Ehsan, "Waste Heat Recuperation in Advanced Supercritical CO2 Power Cycles with Organic Rankine Cycle Integration &

Optimization Using Machine Learning Methods," *International Journal of Thermofluids*, vol. 22, p. 100612, May 2024, doi: 10.1016/J.IJFT.2024.100612.

[34] R. B. Barta, E. A. Groll, and D. Ziviani, "Review of stationary and transport CO2 refrigeration and air conditioning technologies," *Appl Therm Eng*, vol. 185, Feb. 2021, doi: 10.1016/j.applthermaleng.2020.116422.

[35] G. Lorentzen and J. Pettersen, "A new, efficient and environmentally benign system for car air-conditioning," 1993.

[36] G. Lorentzen, "The use of natural refrigerants: a complete solution to the CFC/HCFC predicament," 1995.

[37] P. A. Domanski, D. A. Didion, and J. P. Doyle, "Evaluation of suction-line/liquid-line heat exchange in the refrigeration cycle*t," 1994.

[38] D. M. Nasution, M. Idris, N. A. Pambudi, and Weriono, "Room air conditioning performance using liquid-suction heat exchanger retrofitted with R290," *Case Studies in Thermal Engineering*, vol. 13, Mar. 2019, doi: 10.1016/j.csite.2018.11.001.

[39] J. Wang, D. Qv, Y. Yao, and L. Ni, "The difference between vapor injection cycle with flash tank and intermediate heat exchanger for air source heat pump: An experimental and theoretical study," *Energy*, vol. 221, Apr. 2021, doi: 10.1016/j.energy.2021.119796.

[40] H. Wang, Y. Ma, J. Tian, and M. Li, "Theoretical analysis and experimental research on transcritical CO 2 two stage compression cycle with two gas coolers (TSCC + TG) and the cycle with intercooler (TSCC + IC)," *Energy Convers Manag*, vol. 52, no. 8–9, pp. 2819–2828, Aug. 2011, doi: 10.1016/j.enconman.2011.02.003.

[41] D. Li and E. A. Groll, "Transcritical CO2 refrigeration cycle with ejector-expansion device," *International Journal of Refrigeration*, vol. 28, no. 5, pp. 766–773, Aug. 2005, doi: 10.1016/j.ijrefrig.2004.10.008.

[42] J. Liu, Y. Liu, and J. Yu, "Performance analysis of a modified dual-ejector and dual-evaporator transcritical CO2 refrigeration cycle for supermarket application," *International Journal of Refrigeration*, vol. 131, pp. 109–118, Nov. 2021, doi: 10.1016/j.ijrefrig.2021.06.010.

[43] T. Bai, G. Yan, and J. Yu, "Thermodynamic analyses on an ejector enhanced CO2 transcritical heat pump cycle with vapor-injection," *International Journal of Refrigeration*, vol. 58, pp. 22–34, Oct. 2015, doi: 10.1016/j.ijrefrig.2015.04.010.

[44] M. Á. Gutiérrez, B. P. Pérez, F. D. Muñoz, G. Besagni, and J. M. S. Lissén, "Thermodynamic analysis of an enhanced ejector vapor injection refrigeration cycle for CO2 transcritical operation at low evaporating temperatures," *International Journal of Refrigeration*, vol. 165, pp. 257–276, Sep. 2024, doi: 10.1016/J.IJREFRIG.2024.06.014.

[45] A. R. Raiyan, Samiuzzaman, Y. Khan, M. M. Ehsan, M. R. Karim, and S. M. Siddique, "Exergoeconomic analysis and multi objective optimization of a nuclear driven integrated cooling and power cycle using response surface regression modeling coupled with genetic algorithm," *Energy Convers Manag*, vol. 337, p. 119836, Aug. 2025, doi: 10.1016/j.enconman.2025.119836.

[46] R. H. Mohammed, N. A. A. Qasem, and S. M. Zubair, "Enhancing the thermal and economic performance of supercritical CO2 plant by waste heat recovery using an ejector refrigeration cycle," *Energy Convers Manag*, vol. 224, Nov. 2020, doi: 10.1016/j.enconman.2020.113340.

[47] S. Sadman Bishal, A. Imtiaz Anando, D. Fahim Faysal, and M. Monjurul Ehsan, "Performance Evaluation of a Novel Multigeneration Plant of Cooling, Power, and Seawater Desalination Using Supercritical CO2 Partial Cooling, ME-TVC Desalination, and Absorption Refrigeration Cycles," *Energy Conversion and Management: X*, vol. 20, p. 100485, Oct. 2023, doi: 10.1016/J.ECMX.2023.100485.

[48] S. S. Bishal, D. F. Faysal, M. M. Ehsan, and S. Salehin, "Performance evaluation of an integrated cooling and power system combining supercritical CO2, gas turbine, absorption refrigeration, and organic rankine cycles for waste energy recuperating system," *Results in Engineering*, vol. 17, p. 100943, Mar. 2023, doi: 10.1016/J.RINENG.2023.100943.

[49] M. Pan, X. Bian, Y. Zhu, Y. Liang, F. Lu, and G. Xiao, "Thermodynamic analysis of a combined supercritical CO2 and ejector expansion refrigeration cycle for engine waste heat recovery," *Energy Convers Manag*, vol. 224, Nov. 2020, doi: 10.1016/j.enconman.2020.113373.

[50] A. Yu, W. Su, X. Lin, N. Zhou, and L. Zhao, "Thermodynamic analysis on the combination of supercritical carbon dioxide power cycle and transcritical carbon dioxide refrigeration cycle for the waste heat recovery of shipboard," *Energy Convers Manag*, vol. 221, Oct. 2020, doi: 10.1016/j.enconman.2020.113214.

[51] F. Nanzeeba, T. A. Baigh, A. Kabir, Y. Khan, and M. M. Ehsan, "Genetic algorithm-based optimization of combined supercritical CO2 power and flash-tank enhanced transcritical CO2 refrigeration cycle for shipboard waste heat recuperation," *Energy Reports*, vol. 12, pp. 1810–1835, Dec. 2024, doi: 10.1016/J.EGYR.2024.07.059.

[52] F. Zhang, G. Liao, J. E, J. Chen, E. Leng, and B. Sundén, "Thermodynamic and exergoeconomic analysis of a novel CO2 based combined cooling, heating and power

system," *Energy Convers Manag*, vol. 222, Oct. 2020, doi: 10.1016/j.enconman.2020.113251.

[53] J. Wang, Y. Dai, and Z. Sun, "A theoretical study on a novel combined power and ejector refrigeration cycle," *International Journal of Refrigeration*, vol. 32, no. 6, pp. 1186–1194, Sep. 2009, doi: 10.1016/j.ijrefrig.2009.01.021.

[54] J. Wang, P. Zhao, X. Niu, and Y. Dai, "Parametric analysis of a new combined cooling, heating and power system with transcritical CO2 driven by solar energy," *Appl Energy*, vol. 94, pp. 58–64, 2012, doi: 10.1016/j.apenergy.2012.01.007.

[55] B. Li and S. sen Wang, "Thermo-economic analysis and optimization of a novel carbon dioxide based combined cooling and power system," *Energy Convers Manag*, vol. 199, Nov. 2019, doi: 10.1016/j.enconman.2019.112048.

[56] S. sen Wang, C. Wu, and J. Li, "Exergoeconomic analysis and optimization of single-pressure single-stage and multi-stage CO2 transcritical power cycles for engine waste heat recovery: A comparative study," *Energy*, vol. 142, pp. 559–577, Jan. 2018, doi: 10.1016/J.ENERGY.2017.10.055.

[57] A. Bejan, G. (George) Tsatsaronis, and M. J. Moran, "Chapter 3: EXERGY ANALYSIS," *Thermal design and optimization.*, pp. 113–165, 1996, Accessed: Apr. 29, 2025. [Online]. Available: https://books.google.com/books/about/Thermal_Design_and_Optimization.html?id=sTi2crXeZYgC

[58] F. Zhang, G. Liao, J. E, J. Chen, and E. Leng, "Comparative study on the thermodynamic and economic performance of novel absorption power cycles driven by the waste heat from

a supercritical CO2 cycle,” *Energy Convers Manag*, vol. 228, p. 113671, Jan. 2021, doi: 10.1016/J.ENCONMAN.2020.113671.

[59] A. Lazzaretto and G. Tsatsaronis, “SPECO: A systematic and general methodology for calculating efficiencies and costs in thermal systems,” *Energy*, vol. 31, no. 8–9, pp. 1257–1289, 2006, doi: 10.1016/j.energy.2005.03.011.

[60] L. Zhong, E. Yao, H. Zou, and G. Xi, “Thermo-economic-environmental analysis of an innovative combined cooling and power system integrating Solid Oxide Fuel Cell, Supercritical CO2 cycle, and ejector refrigeration cycle,” *Sustainable Energy Technologies and Assessments*, vol. 47, Oct. 2021, doi: 10.1016/j.seta.2021.101517.

[61] C. Wu, S. sen Wang, X. jia Feng, and J. Li, “Energy, exergy and exergoeconomic analyses of a combined supercritical CO2 recompression Brayton/absorption refrigeration cycle,” *Energy Convers Manag*, vol. 148, pp. 360–377, 2017, doi: 10.1016/j.enconman.2017.05.042.

[62] L. Sun, D. Wang, and Y. Xie, “Energy, exergy and exergoeconomic analysis of two supercritical CO2 cycles for waste heat recovery of gas turbine,” *Appl Therm Eng*, vol. 196, Sep. 2021, doi: 10.1016/j.applthermaleng.2021.117337.

[63] C. Wu, S. sen Wang, X. jia Feng, and J. Li, “Energy, exergy and exergoeconomic analyses of a combined supercritical CO2 recompression Brayton/absorption refrigeration cycle,” *Energy Convers Manag*, vol. 148, pp. 360–377, Sep. 2017, doi: 10.1016/J.ENCONMAN.2017.05.042.

[64] M. H. Nabil, Y. Khan, M. W. Faruque, and M. M. Ehsan, “Thermo-Economic Assessment of Advanced Triple Cascade Refrigeration System Incorporating a Flash Tank and Suction

Line Heat Exchanger,” *Energy Convers Manag*, vol. 295, Nov. 2023, doi: 10.1016/j.enconman.2023.117630.

[65] A. Yu, W. Su, X. Lin, N. Zhou, and L. Zhao, “Thermodynamic analysis on the combination of supercritical carbon dioxide power cycle and transcritical carbon dioxide refrigeration cycle for the waste heat recovery of shipboard,” *Energy Convers Manag*, vol. 221, Oct. 2020, doi: 10.1016/j.enconman.2020.113214.

[66] H. Li, F. Cao, X. Bu, L. Wang, and X. Wang, “Performance characteristics of R1234yf ejector-expansion refrigeration cycle,” *Appl Energy*, vol. 121, pp. 96–103, May 2014, doi: 10.1016/j.apenergy.2014.01.079.

[67] H. Qi, F. Liu, and J. Yu, “Performance analysis of a novel hybrid vapor injection cycle with subcooler and flash tank for air-source heat pumps,” *International Journal of Refrigeration*, vol. 74, pp. 540–549, Feb. 2017, doi: 10.1016/j.ijrefrig.2016.11.024.

[68] A. Mota-Babiloni, J. Navarro-Esbrí, V. Pascual-Miralles, Á. Barragán-Cervera, and A. Maiorino, “Experimental influence of an internal heat exchanger (IHX) using R513A and R134a in a vapor compression system,” *Appl Therm Eng*, vol. 147, pp. 482–491, Jan. 2019, doi: 10.1016/j.applthermaleng.2018.10.092.

[69] Y. Khan, M. W. Faruque, M. H. Nabil, and M. M. Ehsan, “Ejector and Vapor Injection Enhanced Novel Compression-Absorption Cascade Refrigeration Systems: A Thermodynamic Parametric and Refrigerant Analysis,” *Energy Convers Manag*, vol. 289, Aug. 2023, doi: 10.1016/j.enconman.2023.117190.

[70] “Plant Cost Index Archives - Chemical Engineering.” Accessed: May 23, 2025. [Online]. Available: https://www.chemengonline.com/site/plant-cost-index/

[71] X. Wang, Y. Yang, Y. Zheng, and Y. Dai, "Exergy and exergoeconomic analyses of a supercritical CO2 cycle for a cogeneration application," *Energy*, vol. 119, pp. 971–982, 2017, doi: 10.1016/j.energy.2016.11.044.

[72] S. Sanaye, M. Emadi, and A. Refahi, "Thermal and economic modeling and optimization of a novel combined ejector refrigeration cycle," *International Journal of Refrigeration*, vol. 98, pp. 480–493, Feb. 2019, doi: 10.1016/j.ijrefrig.2018.11.007.

[73] V. K. Patel, B. D. Raja, P. Prajapati, L. Parmar, and H. Jouhara, "An investigation to identify the performance of cascade refrigeration system by adopting high-temperature circuit refrigerant R1233zd(E) over R161," *International Journal of Thermofluids*, vol. 17, Feb. 2023, doi: 10.1016/j.ijft.2023.100297.